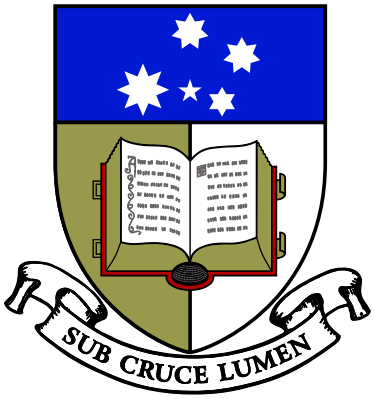


THE UNIVERSITY OF ADELAIDE

# On Using Airborne Optical Vertical Polarisation to Remove Sea Surface Reflectance for Enhanced Visualisation of Seagrass and Other Benthos

Thesis presented for the degree of

Master of Science

David Hart

Bachelor of Arts (Honours) in Geography, The University of Adelaide
Graduate Diploma in Applied Remote Sensing, The University of Adelaide
Graduate Certificate in Public Sector Management, Flinders University

July 2009

Faculty of Sciences, Discipline of Soil and Land Systems

# 1 Introduction

## 1.1 Introduction

Mapping of marine benthic flora using remote sensing techniques has, over the past decade, been used to locate environmentally stressed areas in the South Australian marine environment (Seddon 2002, Hart 1995, Hart 1997, Hart and Cameron 1998, Cameron 1999a, Cameron 1999b, Hart 1999, Cameron and Hart 2002a, Cameron and Hart 2002b, Hart and Clarke 2002, Cameron, Hart and Clarke 2002, Cameron 2003, Cameron 2008a and Cameron 2008b). These studies used panchromatic/colour aerial photography and/or medium resolution multispectral satellite imagery to create a time series showing location and rate of seagrass loss. While successful within their project parameters, these studies were limited by conditions at time of image capture, such as sun-glare, turbidity, wave action and low contrast in deeper waters due to absorption and scattering. This research thesis investigates the use of polarisation as a method to minimise these limiting factors.

## 1.2 Research Aims

This study has two aims. The first is to investigate the use of polarisation, in conjunction with light intensity and wavelength, as another information source in the remote sensing of marine benthic flora.

The second research aim is to use polarisation to remove surface reflection from optical (visible to near infra-red) aerial photography and to better detect seagrass beds in coastal waters.

## 1.3 Importance

Seagrasses are recognised as an important part of South Australian ecosystems (Deans and Murray-Jones 2002). Traditional aerial photography is still the recommended method for mapping seagrass beds even though there are severe problems with the interpretation of film based imagery (McKenzie et al. 2001). There has been very little research into use of the other non-spectral properties of photons such as polarisation in remote sensing (Egan 1985). Therefore the importance of this

study is that it extends the data sources available for mapping seagrasses and directly demonstrates this improved technique.

## 1.4 Background

Seagrasses and other marine benthic flora are recognised as an important part of the South Australian environment (Baker 2004), so much so that it is currently an offence to remove or interfere with aquatic or benthic flora (or fauna) of any waters without a permit (see *Fisheries Act 1982: Section 48G)*. This prohibition includes the wrack or beachcast phytodetrital matter washed up on the shore[1]. This prohibition is due to the recognition of the influence of marine flora on terrestrial ecosystems (Kirkman and Kendrick, 1997, Orr et al. 2005). The conflicts between marine conservation and marine development sometimes spill over into the Environment, Resources and Development Court of South Australia, where development applications for aquaculture using oyster leases or tuna cages have been opposed due to perceived impacts on seagrasses. There is much public and parliamentary debate on proposed Marine Protected Areas. Much of this is due to a perceived poor understanding of marine benthic flora[2] and of human-induced impacts due to development, both terrestrial and marine, and to impacts due to changing climate (Edyvane 1999, Short and Neckles 1998). Numerous workshops and seminars have occurred in South Australia (Cugley 1997, Butler et al. 1997a, Butler et al. 1997b, Butler et al. 1997c, Seddon and Murray-Jones 2002) leading up to the recently completed Adelaide Coastal Waters Study (Fox et al. 2007).

The well-documented loss of seagrass along the Adelaide metropolitan coastline (Neverauskas 1987, Hart 1997, Environment Protection Agency 1998) differs from the pattern of loss found in other marine environments (Westphalen et al. 2004). Other study sites around the world have found loss mainly in the light-poor deeper water areas, where decreases in the intensity of light reaching the leaves is the prime cause of loss. The loss of near-shore seagrass off Adelaide indicates the stressors are not primarily related to the quantity of light, but other environmental factors. These are possibly related to land-based discharges and epiphyte growth, but

[1] An example of permission to collect wrack, see the South Australian Government Gazette of 24 January 2005, p24.

[2] Even as recent as 2004 four new species of marine benthic flora were described in Southern Australian Waters (Womersley, 2004), mainly deep water marine algae.`

studies are inconclusive (Harbison and Wiltshire 1997, Environment Protection Agency 1998, Seddon 2002). Recent studies indicate that the loss may be due to differential responses to stress by *Posidonia* and *Amphibolis*, in that once *Amphibolis* is lost, the natural recolonisation processes (Cambridge 1975) are suspended. However seagrass changes far from shore may also be occurring, but not monitored due to the difficulty of seagrass/ sand discrimination in deeper waters using current sensors.

Remote sensing has been used in the past to delineate seagrass change, and has the potential to be used for monitoring future changes. Aerial photography remains the sensor of choice for seagrass mapping (McKenzie, et al. 2001). However traditional methods have not been completely successful for a variety of reasons. Chapter 2 points out the strengths and weaknesses of current methods, and more specifically in the context of the South Australian marine environment.

## 1.5 Thesis Structure[3]

Chapter 1 introduces the background of the research, and its importance in the South Australian environment.

Chapter 2 outlines the current knowledge about seagrasses, concentrating on their presence in the South Australian marine environment and previous *in-situ* studies. This chapter reviews remote sensing studies on seagrasses and discusses the strengths and weaknesses of different methodologies and techniques. It then explores the theory behind using polarisation for remote sensing of marine benthic flora. The background of the initial experimental design prior to image capture is presented. Two image acquisition flights were conducted. The first was a pilot experiment to test the methodology, whilst the second captured experimental imagery for this thesis.

Chapter 3 covers the pilot experimental design, data capture, findings and discussion and factors that were taken into consideration in the final experimental design.

[3] Footnotes are used where additional information is added for completeness.

Chapter 4 describes the revised experimental design and the null hypothesis for the research is introduced. The image capture sortie is described and the results of the polarisation experiment with selected examples are given. A discussion on the findings and the disproving of the experimental null hypothesis, within certain experimental constraints is presented. The significance of this experiment and findings are explored.

Chapter 5 summarises the thesis findings and presents further improvements of the experimental design and directions for future research.

Appendix 1 records the environmental conditions up to and during the experiment that may be of interest to meteorolophiles.

Appendix 2 compares a series of co-temporal horizontal and vertical polarisation frames captured on the experimental flight, showing the differences in benthic detail at, and away from, the Brewster angle.

Appendix 3 is a conference paper: "David Hart**,** Megan Lewis, Paul Dare, Bertram Ostendorf (2006) Seeing seagrasses sidewards: Marine angiosperms and the Stokes' polarization parameters, proceedings *13th Australasian Remote Sensing and Photogrammetry Conference,* Canberra ACT, 20-24 November 2006."
This paper summarizes the research outlined in the first two chapters of this thesis.

Appendix 4 is a conference paper: "David Hart**,** Megan Lewis, Bertram Ostendorf (2008) Stripping away sky reflectance, waves and turbulence for benthic mapping: Imaging the seafloor not the surface, proceedings *14th Australasian Remote Sensing and Photogrammetry Conference,* Darwin NT, 29 September – 3 October 2008."
This paper summarizes the progress outlined in chapter 4 of this thesis and presented some initial findings.

# 2 Review of previous studies

## 2.1 Introduction

Thomas, et al. (1999) states that *"[remote sensing seagrass studies] will be successful only if they combine highly developed expertise in remote sensing with equivalent knowledge of the ecology and environmental characteristics of the target site."* With this in mind, this review examines the characteristics of marine benthic flora, compared to terrestrial flora, to gain an understanding of the target subject, and an overview of its contribution to the South Australian marine environment. It then briefly reviews the history of seagrass studies, leading to the remote sensing and mapping of marine benthic flora, with a more detailed census and critical examination of past studies off the South Australian coastline.

The core of the review is an overview of current methods and current research into the remote sensing of marine benthic flora. This is designed not as a complete census, but as a discussion highlighting current problems and challenges.

## 2.2 Characteristics of Marine Benthic Flora

Benthic flora, both seagrasses (marine angiosperms) and macroalgae, have several characteristics that are radically different to terrestrial plant species. As seagrasses are related to terrestrial and freshwater aquatic angiosperms, a comparison of seagrasses with non-marine angiosperm species will highlight important differences due to seagrass adaptation to the marine environment. These characteristics, apart from the aquatic nature of the environment that will be dealt with separately, have direct and indirect influences on the selection of remote sensing sensors and analysis techniques.

## 2.3 Seagrasses

Seagrasses are marine-only flowering plants[4] believed to be descended from ancestors that recolonised the sea 90 to 120 million years ago (Enriquez 2005 for

[4] Division Magnoliophyta (Angiosperms), Class Liliopsida (Monocotyledons) (Kuo and den Hartog 2001).

Den Hartog). There exist around 60 known species of seagrass in the world in 12 genera and 4 families[5], as of 2001 (Short and Coles 2001), though genetic testing may alter these numbers in the near future (Short et al. 2007). These species are grouped into six bioregions worldwide (Short et al. 2007). Compared with terrestrial and fresh water submerged aquatic angiosperms this biodiversity is relatively low (Stevenson 1988)[6]. All seagrasses are monocots (Stevenson 1988).

Seagrasses are highly clonal, having advantages of anchorage and biomass storage in the matte[7] (sheaths, roots, rhizomes together with accumulated sediment; Pergent et al. 1997, Zupo et al. 2006), though with the disadvantage of being genotypically depauperate. For example in the Tyrrhenian Sea, west of Italy, many sites studied are uniclonal or show evidence of inbreeding and low genetic diversity (Procaccini et al. 2001). In terms of southern Australian conservation management, individual *Posidonia australis* meadows have not been found to be genetically uniclonal due to recruitment into new and existing meadows, but do have low genetic diversity (Waycott 1998). This has implications for management of genetic diversity when selecting boundaries for marine protected areas, as some patches would be more diverse than others. This low genetic diversity means that seagrasses could be subject to die-offs due to environmental extremes (Seddon et al. 2000). Any apparent gain in seagrass extents observed in imagery would be due to infilling within existing subtidal seagrass beds (either clonal or new plants), detrital matter or macroalgae (Hart 1997).

Although seagrasses use mainly clonal strategies, they do sexually reproduce through the production of fruit, seeds or viviparous seedlings. However there is a limited spatial dispersal strategy employed by most seagrasses. For example, in tropical Australia, the similarity of unstable marine sands to physically dynamic desert sands has resulted in similar seed dispersal strategies between arid-lands plants and

[5] 13 genera and 5 families if *Ruppia* is included. Kuo and den Hartog (2001) excludes the family Ruppiaceae as being part of another ecological group, the poilkilosaline aquatic plants, whereas Robertson (1984) and Short et al. (2001) include them as the term seagrass should include all angiosperms that reproduce in the sea. *Ruppia* was found in the Coorong (Robertson 1984) but is now believed to be locally extinct (Brenton Greer, DEH, *pers comm.* 2004).

[6] Worldwide there are around 500-700 species of freshwater and estuarine submerged angiosperms compared to 60 marine angiosperm species.

[7] The literature is ambiguous as to the term for the dense rhizome/sediment mass that occurs below seagrass meadows, and remains after the living seagrass has vanished. Refereed literature tends to use the term ‘matte’, whereas Seddon et al. 2003 use the term ‘fibre mat’.

seagrasses. Sheltered micro-habitats such as found in existing seagrass meadows such as *Halodule uninervis* are preferred over colonising bare locations (Inglis 2000). This means that seagrasses that produce dormant seeds use a restricted seed dispersal strategy (atelechory or a lack of seed dispersal characteristics[8]), so that once seagrass is lost from an area then the probability of recolonisation by seeds from other nearby sources is low (Piazzi, et al. 1999). This may explain the low genetic variability found in seagrasses in general, as new areas of colonization would be the result of a genetic bottleneck, as seen with the recolonisation of the fucoid algae *Fucus serratus* in Northern Europe after the last ice age (Coyer, et al. 2003) and *Posidonia australis* in Shark Bay Western Australia (Waycott 1998).

Other adaptations to the marine environment include the loss of stomata, the development of a photosynthetic epidermis, and an unpigmented mesophyll containing large vacuoles (Enriquez 2005). This placing of the leaf pigment in a single epidermal layer means easier access to bicarbonate, the main inorganic source of carbon in seawater, plus the mesophyll scatters light back to the pigment. The photosynthetic pigments are closer to the external light, possibly as a response to low light conditions. In this regard it should be noted that many seagrasses have little built-in defence against damage by high-energy photons such as ultra violet light (usually UV-B), relying on the screening effect of the water layer and attached periphytes[9] (Brandt and Koch 2003). This results in susceptibility to blanching damage. Seagrasses that are intertidal rely on ultra-violet defence mechanisms similar to terrestrial plants. These adaptations suggest that seagrasses need to avoid shallow waters at low tide.

Seagrass is subject to photic stress due to both microalgal and macroalgal growth. These algal blooms are due to enriched nutrients reaching the normally nutrient poor coastal waters from terrestrial sources. These can take the form of epiphytes which, as well as shading the seagrass leaves, cause oxygen depletion and increased turbidity (McGlathery 2001). The amount of epiphytes can be species dependent; in American River, South Australia *Posidonia* has been noted for the wealth and range of epiphytes, whereas *Zostera, Halophila and Lepilaena* have much fewer epiphytes

[8] Though many South Australian seagrasses produce floating seeds, eg *Posidonia australis* blow-outs are usually colonised by clonal *Amphibolis antarctica* (Shepherd and Sprigg 1976).

[9] Periphyton: complex matrix of underwater algae and heterotrophic microbes firmly attached to solid surfaces such as rocks and plants.

(Womersley 1956). This epiphyte coverage will hide the signature of the seagrass from any above-water sensor.

## 2.4 Macroalgae

Marine macroalgae are known in a greater number of species than seagrasses. As an example of macroalgae species diversity one deep water transect study of the upper Spencer Gulf identified four species of green algae (Chlorophyceae), eighteen species of brown algae (Phaeophyceae), fifty-one species of red algae (Rhodophyceae) and seven species of seagrasses (Shepherd 1983). Even as far back as 1929 a study of the known published records found twenty-nine species of green algae, sixty-one species of brown algae, and two hundred and fifty species of red algae in South Australian waters (Lucas 1929). Today over eleven hundred species of macroalgae have been described (Womersley 2004).

Macroalgae use several different pigments for photosynthesis, usually adapted to depth[10]. The green and brown algae are usually found close to the sea surface, whereas red algae are more commonly found at depth, at least in South Australian waters (Womersley and Edmonds 1958). It has long been known that spectral differences due to various amounts of different pigments are indicative of different types of macroalage (Stokes 1852). Chlorophyll a is found in all plants, algae and cyanobacteria, and so can be taken as a base chemical absorption and reflectance signature. Chlorophyll b is found in green algae and marine angiosperms. Carotenoids, being able to absorb a wide range of energies, albeit not always with high efficiency (Raven and Johnson 1986), usually increase with low-light conditions at depth in some macroalgae (Perez-Bermidez et al. 1981). Fucoxanthin is found in brown algae (kelps) mainly as a protection against harmful light at the sea surface, and as complementary spectral adaptation to the ambient light field at depth (Perez-Bermidez et al. 1981). Other common algal pigments include phycocyanin, found in blue-green algae, phycoerythrin in red algae, and the phycobilins, found in cyanobacteria and the macroalgae rhodophyta. In terms of reflectance these pigments have characteristic colours. Chlorophyll a absorbs red, and so appears blue-green. Chlorophyll b absorbs blue, and so appears yellow-green. Carotenes

[10] Even the scientifically literate public knew this in the 19th century. Jules Verne in *Twenty Thousand Leagues Under the Sea* p 114 had the main character correctly comment "*I noticed that the green plants kept nearer the top of the sea, whilst the red were at a greater depth, leaving to the black or brown the care of forming gardens and parterres in the remote beds of the ocean*."

appear orange, fucoxanthin appears brown, phycocyanin appears blue, and phycoerythrin appears red (Kelly et al. 1987).

Macroalgae use their attachment to the substrate as an anchor rather than root system. This means that sessile macroalgae are found attached to reefs, rocks and shells, and generally avoid soft substrates such as sand or mud (Womersley 1956). This can result in a spatial separation between seagrasses and macroalgae based on the type of substrate (Johnston and Mawson, 1946). This may have implications for image segmentation of seagrass or macroalgae dominant regions based on mapping of benthic substrates from bottom sampling or soil reflectance.

## 2.5 Biogeography and Ecological Significance of South Australian Marine Benthic Flora

Marine benthic flora are found in areas were certain environmental conditions are met. These conditions include soft substrate for seagrasses and hard substrate for macroalgae, sufficient light for photosynthesis, but not too much light or heat near to the shore. South Australia has large areas of shallow coastal environments, mainly in bays on western Eyre Peninsula, Spencer Gulf and Gulf St Vincent, Kangaroo Island and the south-east Limestone coast region.

For seagrasses optimal conditions are found along much of the South Australian shore environment, from near the Head of Bight in the west, through the bays and gulfs, to the southernmost coast near the Victorian border. Being native to the South Australian coastal environment, seagrasses are an essential part of the marine ecosystem (Deans and Murray-Jones 2002).

Seagrasses are important nursery areas for commercially and recreationally fished fish species, such as King George whiting (*Sillaginodes punctatus)*. Seagrasses have a role in sediment stabilisation and onshore wave refraction. The example of the loss of seagrasses at Beachport in south-eastern South Australia has meant that the waves are now scouring the beach at an angle compared to fifty years ago when the waves refracted to break parallel to the beach resulting in little along shore movement. The sediments previously protected by seagrass have been eroded, deepening the offshore bathymetry (Seddon et al. 2003).

## 2.6 Evidence of Seagrass in South Australian Waters

In South Australia seagrass has become an environmental and politically iconic vegetation community. No other marine benthic flora has achieved this public recognition. While seagrasses do play an important role in marine ecosystems and marine substrate stability, the popular view is such that what is good or bad for seagrass is seen as good or bad for the general marine environment. However what evidence is there that seagrasses have been a long-term widespread part of South Australian marine ecosystems? The evidence suggests that seagrasses may have been established since at least the middle Eocene, but the further back in time one investigates the less direct the evidence. This section reviews the historic and geological evidence for seagrass presence in South Australian coastal waters.

Seagrass meadows were a natural part of the Holocene South Australian marine environment. An example of direct evidence of this is in the form of a layer of *Posidonia* fibres in a core sample collected near Robe dating between 7500BP to 2000BP. Fossil molluscs (*Katelysia* spp.), which today are found in intertidal and subtidal seagrass meadows, plus fossil foraminifera *Discorbis dimidiatus* and *Elphidium crispum* which exist in environments conducive to seagrass, were found in this and other core samples, indirectly indicating the presence of seagrass meadows (Cann et al. 1999). The upper Spencer Gulf has distinct Holocene deposits of *Posidonia australis* dating back to 6600BP (Belperio et al. 1984) with Pleistocene formations showing similar patterns and processes indicative of seagrass (Gostin et al. 1984).

Further indirect evidence suggests that seagrass environments may have existed in the Middle Eocene in the St Vincent Basin, where fossil bryozoans similar to *Densipora corrugata* and *Cellepora cristate*, which currently are found growing on *Amphibolis*, have been found in Tortachilla Limestone (James and Bone 2000). Likewise the presence of seagrass dwelling foraminifera such as *Marginopora* and *Cyclogyra* in Oligo-Miocene Murray Basin marine deposits, together with external moulds of seagrass blades on bryozoans, indicates extensive seagrass beds in the shallow seas of the time (Lukasik et al. 2000). The sediment depositional properties of seagrass meadows may have resulted in the terrigenous silt and clay deposits found in these geological layers.

Macroalgae, being mainly soft-bodied, tends to leave very little in the fossil record, apart from coralline red and green algae. There is little direct geological evidence in southern Australia, so that like seagrass, the inference for soft-bodied macroalgae is based on indirect evidence such as similar assemblages (Domning 1981). Coralline deposits are more promising, with fossils of red and green algae found in Oligo-Miocene and Pliocene Murray Basin marine layers (Lukasik et al. 2000, Pufahl et al. 2004).

Early historical references to seagrass in South Australian waters are scarce, with most references to observations of the sea floor mainly concerned with depth or ship draught, shoals and bars, or suitability for anchorage. However some clues exist, as benthic flora was actually to be avoided for anchorages, with sand or mud preferred. This was due to fouling of the anchors if weather conditions worsened and the ship dragging the anchor (Sturt 1847). A few direct references do exist. For example, Baudin in his survey in 1803 of Murat Bay off present day Ceduna noted the presence of underwater grasses (Hasenohr 2000) and on the same voyage Peron noted grasses in Nepean Bay, Kangaroo island (Peron 1816). Likewise Colonel Light in 1836 noted "*mud and weeds*" in 3.5 fathoms of water off the Patawalonga River at Glenelg (Harbison 2002).

Botanists naturally were more cognisant of marine flora. By 1914 *Ruppia, Zostera* and *Posidonia* were known to form submarine meadows off Adelaide and other sheltered areas, and the wrack "… *lines the foreshore from Outer Harbor to Brighton with a belt of "sea weed" some yards across and 18in. to 2ft. deep.*" (Osborn 1914)[11]. Griffith in 1913 pointed out that *Amphibolis "… grows beyond low-water mark at Henley Beach, and is often cast up on the shore."* (Black 1913) showing that the later near-shore loss of seagrass had a large *Amphibolis* component[12].

South Australian marine algae were heavily collected and identified by this time. In 1929 a census of records of *"… South Australian Marine Algae, Green, Brown and Red…"* showed a total of 340 species collected from South Australian waters (Lucas

[11] Though there was confusion in this report over the identification of *Amphibolis antarctica*, variously labelled *Cymodocea* (Tepper 1882, Ascherson, and Tepper 1882) or *Pectenella* (Black 1913).

[12] Even in 1946 it was noted that off Noarlunga "… *Where the seafloor consists of rather firm sand, Zostera Muelleri and Cymodocea* [sic] *antarctica occur. Posidonia australis prefers deeper water.*" (Johnson and Mawson 1946).

1929). This resulted in the first books on South Australian seaweeds (Lucas 1936, Lucas and Perrin 1947).

Later studies mapped the intertidal marine ecology down to the seagrass beds (Womersley 1956, Womersley and Edmonds 1958). Since the development of scuba diving there have been many in-depth studies of the deeper marine environment in South Australia. There have been several dive-based studies of benthic flora and habitat, such as Gulf St Vincent (Shepherd and Sprigg 1976), Pearson Island (Shepherd and Womersley 1971), St Francis Island, (Shepherd and Womersley 1976), Waterloo Bay (Shepherd and Womersley 1981), West Island (Shepherd and Womersley 1970, Cheshire et al. 1996) and Upper Spencer Gulf (Shepherd 1983). These produced maps based on, and interpolated from, dive point and transects, though the Waterloo Bay study did use hardcopy aerial photography as an adjunct in areas down to depths of 4 metres.

In summary, the direct written evidence puts seagrasses firmly as part of the South Australian marine environment at least since 1803, and by inference well before 1803. Lack of observations by some early explorers and settlers could be due to a lack of botanical knowledge, and the habit of grouping all marine floras as seaweeds. Recent Holocene formations show direct geological evidence from the time when the last major marine transgression in widely separated South Australian coastal locations occurred. Further back the evidence seagrass is indirect, based on indications of similar environments and fossil species associations as today. It is safe to conclude that seagrasses have been a prevailing part of the South Australian marine environment.

## 2.7 Previous Remote Sensing Studies of Benthic Flora

### 2.7.1 Early Studies

Mapping of seagrass extents in certain regions has been undertaken since before aircraft-based aerial photography. These studies used dredging and other bottom sampling techniques. In one study of successive seagrass mapping near Marseilles, France, from 1883 to 2000, the original maps, and later versions, have been found to be of variable and even questionable accuracy (Leriche et al. 2004).

Aerial photography has been captured specifically for benthic flora mapping since the late 1940's. Examples of such surveys include Nova Scotia (Cameron 1950), US Virgin Islands (Kumpf and Randall 1961), Bahamas (Kelly and Conrad 1969) and New Zealand (Steffensen and McGregor 1976). Panchromatic, colour and false-colour infra-red film was used with different lens filters. These were mainly empirical approaches, with only limited discussion of water and vegetation absorption and reflectance properties. Photography was manually mosaicked and rectified to available terrestrial mapping. Interpretation generally employed normal photo interpretation techniques using prints or the original negatives back-lit, sometimes in stereo. Satellite colour photography was used in the 1960's (Kelly and Conrad 1969) derived from astronaut hand-held cameras. One common theme, apart from the satellite photography, is the large scale of the photography used, usually in the 1:4000 to 1:25000 range (and the often stated recommendation for satellite photography is for a higher spatial resolution).

Medium resolution multispectral satellite imagery has been used in benthic mapping with apparently good results. Not many early studies exist, probably due to the low resolution of Landsat MultiSpectral Scanner (MSS) and the lack of good radiometric resolution (7-bit or 128 grey levels) in the green band. For example one study masked out all areas that where optically deep due to deeper water increasing apparent percent canopy cover and causing classification errors (Ackleson and Klemas 1987). Once Landsat Thematic Mapper and SPOT data were available many more studies were undertaken up to the present day.

### 2.7.2 Australian Studies

In Australia the use of historical aerial photography has a similarly long history. Local seagrass change studies such as in Moreton Bay, Queensland 1942-1975 (Kirkman 1978), Cockburn Sound, Western Australia 1954-1978 (Cambridge and McComb 1984) and in Botany Bay, New South Wales 1930-1987 (Larkum and West 1990) all used unrectified aerial photography. Off Rottnest Island, Western Australia (Hastings et al. 1995) a study of seagrass damage associated with boat moorings between 1942 and 1992 used unrectified stereo pairs of photographs for interpretation. Each of these studies transferred the interpretation into a spatial context by best-fitting the hardcopy interpretation onto existing maps. Later studies, such as in Cockburn Sound, Western Australia, 1967-1999 (Kendrick et al. 2002) used ortho-rectified

aerial photography to look for change. No indication of correction for refraction is mentioned in any of the above studies.

The use of medium resolution satellite sensors has been limited, possibly due to the coarse resolution compared to aerial photography when measuring change over time in local studies. However, the method has been used for single date (as opposed to multitemporal, see Ippoliti-Ramilo et al. 2003) regional mapping in Australia. For example Landsat TM band 1 hardcopies have been used in conjunction with dive samples to map seagrass and substrate in Western Australia, South Australia and Victoria, released as a series of regional reports (eg Edyvane and Baker 1999). In another example, Lonsdale Bight in Port Phillip Bay was mapped using Landsat TM bands 1 and 2, with the infra-red bands used to define the landward edge (McGoldrick and Leach 1998). Seagrass and macroalgae change detection using Landsat imagery over Wallis Lake, New South Wales was successful at the broad (multi-pixel) level but not at the individual pixel level (Dekker et al. 2005). These studies showed that, while fulfilling the requirements of the studies, the small number of useful bands is a limitation. This limitation carries across to SPOT and ASTER, which do not have bands in the blue part of the spectrum.

The above studies are available in the peer-reviewed literature. However there are a large number of non-refereed, non-published reports, referred to as grey literature, which exists as private sector or government agency consulting reports (Thomas et al. 1999). However trends and gaps can be found. Thomas et al. (1999) in their review of monitoring and assessment of seagrass found several weaknesses with current methods. These will be detailed in the sections outlining individual sensor types.

### 2.7.3 South Australian Studies

Uncorrected aerial photography has been used, and is still being used, to delineate seagrass change in South Australia with approximate locations. Seagrass diebacks due to natural and human induced causes have occurred in South Australia in recent times. Similar to the North Atlantic seagrass dieback in the 1930's (Cotton, 1933) there was a natural dieback in the Upper Spencer Gulf in 1993 (Seddon et al. 2000), though due to environmental stress rather than disease. Human induced diebacks have occurred, some of which can be directly related to a cause, such as increased

nutrient load due to treated sewerage outfall off Point Malcolm (Neverauskas 1987a, Bryers and Neverauskas 2004), and others where it is more difficult to pin-point the cause, such as Beachport (Seddon et al. 2003).

While unrectified aerial photography was sufficient for mapping, the need for rectified, or better still orthorectified, aerial photography was recognised for better accuracy of delineation and was especially critical for change detection analysis. Ortho-corrected aerial photography has been used since 1994 to map seagrass extents in South Australia to a higher positional accuracy. The first pilot study off West Beach/ Glenelg North successfully used orthorectified aerial photography from 1949 through to 1994[13] (Hart 1995). One innovation was the use of refraction correction based on manipulation of the bathymetric digital elevation model (Gibson 1995, Evans and Acikgoz 1986). This study was later expanded to cover the Largs Bay to Aldinga Beach area (Hart 1997, Hart and Cameron 1998). This same photography was used in the Adelaide Coastal Waters Study (Blackburn and Dekker 2006) and did confirm earlier mapping. Further studies in Port Lincoln Proper/ Boston Bay (Hart 1999), off the mouth of Cygnet River on Kangaroo Island (Cameron and Hart 2002a), and Beachport (Hart and Clarke 2002, Cameron 2008b) used a similar methodology, apart from the discontinued use of refraction correction in later studies.

There are severe limitations to this method. None of the historical photography was flown for seagrass mapping *per se*, so the camera and film processing settings were for terrestrial features. The exposure settings were not set for low light conditions. In terms of successful terrestrial photography acquisition, calm water surface conditions, lack of sun glare and turbidity were not critical factors. Often the coastline was where the camera was turned off and the aircraft turned to start a new run, so that there is limited coverage offshore.

Positionally, even though elevation corrected and refraction corrected, the mapping accuracies were relatively poor compared to terrestrial orthophotography. The natural-feature control used was purely terrestrial, and so the orthophotographs were extrapolated out to sea (though Pasqualini et al. 1997 and Leriche et al. 2004 used similar terrestrial-only control and extrapolation methods). When used for change detection this could give a mismatch between epochs of photography leading to

[13] Aerial photography dates: 10/1/1949, 3/1/1959, 5/2/1965, 15/5/1977, 17/4/1983, 11/11/1988 and 2/2/1994

apparent change rather than real change (sliver effect[14]). Because the classification methodology for the Adelaide metropolitan coast was designed to minimise this effect (similar to minimising the effects of detrital matter between epochs), the detection of any gain in benthic flora was not possible using this method. In other areas of South Australia away from the metropolitan Adelaide coastline the correction for refraction was deemed unnecessary due to the control and bathymetric digital elevation model accuracies being much poorer than any error corrected for by the refraction algorithm.

Despite these limitations there are direct correlations between the above findings and other independent non-imagery studies. A correlation between area of sand gain along the Adelaide metropolitan coastline (Hart 1997) and the volume of sand erosion/ deposition was shown by Fotheringham (2002). The extra sand areas (seagrass loss) prior to 1970 were the result of sand deposition north of Glenelg, whereas the extra sand areas post 1977 were due to erosion south of Glenelg. As well the seagrass loss and transport onshore of sand explained a previously unexplained input of 120000 – 140000 $m^3$ of sand in the sediment budget north of Glenelg. Unstable movement of sand was the cause of seagrass loss by burial in Moreton Bay, Queensland between 1942 and 1975 (Kirkman 1978). The Beachport seagrass study (Hart and Clarke 2002) correlated seagrass loss with beach profiles showing seabed erosion (Seddon et al. 2003).

Other regional-scale studies have used medium resolution satellite imagery. Edyvane and Baker (1999) used GPS-located dive points with Landsat TM band 1 imagery to map benthic habitat. Later studies used time series Landsat Thematic Mapper imagery in the Upper Spencer Gulf (Cameron, 1999a) and Gulf St Vincent (Cameron 1999b) to map seagrass change. The results were ambivalent at best, as the low resolution meant that spatially significant changes needed to occur to be able to be detected on the imagery. High resolution Quickbird imagery was used in the Adelaide Coastal Waters Study (Blackburn and Dekker 2006), though the end result was similar to aerial photography.

In conjunction with the Cygnet River study (Cameron and Hart, 2002a) a multi-temporal and multi-sensor study of Nepean Bay, Kangaroo Island used Landsat TM,

[14] Misaligned pixels where the apparent change is due to an area of substrate in one epoch is in the same location of an area of seagrass in another epoch, or *vice versa*, whereas no change has in effect happened.

orthorectified aerial photography and ASTER imagery, together with a logical key was used to find remnant seagrass amongst macroalgae communities (Cameron and Hart, 2002b). The macroalgal bloom off the mouth of the Cygnet River, Kangaroo Island is due to nutrient run-off, which is in turn due to farm fertilizer use in a terrestrial naturally nutrient-poor environment (Lewis 1921). This macroalgal bloom has been seen, initially using local knowledge and confirmed by remote sensing techniques, to be at the detriment of the seagrass meadows in Nepean Bay (Edyvane, 1997, Cameron et al. 2002).

There has been a range of seagrass hyperspectral studies in South Australian waters. These match the detailed spectral signatures of marine features with those in the imagery. Though showing promise, the pre-processing and sampling necessary for correct identification means there is a large overhead involved (Anstee et al. 2000, Anstee et al. 2006, Dunk and Lewis 2000, Treilibs et al. 2006, D. Blackburn *pers comm*. 2005). The remote sensing component of the Adelaide Coastal Waters Study used Compact Airborne Spectrographic Imager (CASI) imagery to map percentage cover of several species of seagrass (Blackburn and Dekker 2006). The main advantage over earlier methods was the amount of spectral detail for feature discrimination and water column measurements. As with other methodologies the sea-surface conditions need to be calm and the water column of low turbidity.

## 2.8 Current Benthic Image Acquisition Methods

There are many systems and sensors for remote sensing of benthic flora. The section on previous remote sensing studies of benthic flora (see above) has described past studies. This section details the strengths, weaknesses and possibilities of each sensor type.

### 2.8.1 Aerial Photography

Traditional film based aerial photography is still being used for benthic mapping, and is seen as the current recommended technology (McKenzie et al. 2001). Usually there is no choice for historical studies of change over time as aerial photography is the only high-resolution imagery available (Hart 1995). A stronger reason is the cost effectiveness of aerial photography compared to other current imagery sources

(Mumby et al. 1999). For small localised studies the resolution is better than most satellite imagery (for example Chauvaud et al. 1998).

There are several weaknesses of film based aerial photography for seagrass mapping. Due to absorption and scatter, over water the image is usually darker compared to land except in the blue/green part of the spectrum. This can be adjusted for when planning and executing the aerial photography capture. To bring out detail in the water exposures need to be longer or with a wider aperture than over land. Once exposed, the film can then be scanned, with the gamma[15] adjusted to bring out more information in the darker regions. The film can be scanned at a higher radiometric resolution to bring out more detail. However aerial photographic film, until recently, had intrinsically a low dynamic range, and early photography when scanned at 16-bit gave little more information than 8-bit[16]. 16-bit images tend to bring out a large degree of noise rather than an improvement in signal. This is due to the Modulation Transfer Function (MTF) of film, which is the relationship between contrast and resolving power. High contrast features are resolved at smaller sizes than low contrast features. The negatives when scanned at 16-bit can exhibit Newton's rings in dark, low-contrast areas such as water. This results in classification problems when using historical aerial photography. This can only be eliminated by the use of expensive anti-Newton ring glass both above and under the film layer when scanning. The later aerial films such as Kodak 2444 (Eastman Kodak Company 2001) do have better than 8-bit radiometric resolution per band and can be used to push the interpretation into deeper darker waters.

The spectral response of film is very wide in the visible and near infra-red, with broad and overlapping spectral sensitivity for each of the blue, green, red and especially near infra-red sensitive dyes (Eastman Kodak Company 2001). Aerial photography colour film is designed to mimic the response of the human eye. It is not designed to have narrow spectral sensitivity. Therefore traditional remote sensing spectral classification techniques tend to work poorly when applied to scanned film (London 2004). That said there has been successful mapping of intertidal seagrass using scanned and orthorectified infra-red film (Young et al. 2008).

[15] Gamma is the slope of the relationship which maps the input scanned values to the output digital number.

[16] The bit size is the amount of radiometric discrimination per band. In terms of digital data storage 8-bit is one byte, or 256 grey levels, and 16-bit is two bytes, or approximately 16.7 million grey levels.

The positional accuracy of unrectified aerial photography is low. This is because of the distortions due to topography in central perspective images[17]. All elevated features are displaced away from the principal point in proportion to distance from the principal point and height of the object. This can be exacerbated by tips and tilts of the camera, moving the principal point away from the nadir position. Due to the central perspective nature of the imagery, any tips, tilts or height displacement can cause mismeasurement of change. This can result in up to 100% overestimate of change even with polynomial rectification (Rocchini 2004). The solution of course is orthorectification where most of the displacements due to height differences are removed (Hart 1995, Young et al. 2008).

One improvement over the use of terrestrial-only ground control is the use of differential Global Positioning System/ Inertial Measurement Unit (GPS/IMU) systems on aircraft. This gives, to a certain level of accuracy, all six orientation parameters (easting, northing, height, omega, phi, kappa[18]) that when used in an aero-triangulation software package can bridge between opposite shorelines. Therefore control is only needed on both coastlines. This has been proven operationally in the upper Spencer Gulf (DWLBC 2009).

The use of polarized aerial photography has been surprisingly limited. Long et al. 1994 used a hand-held Hassleblad camera with a blue polarizing filter. However no reason was given for the choice of filter nor whether it improved results. Studies have been undertaken using polarized filters on hand-held cameras in aircraft for soil surface moisture and vegetation amount (Curran, 1978, Curran 1979, Curran 1981). These have found positive correlations between polarisation and the ground variables measured. However other methods such as the use of false-colour infra-red film give more accurate results than the use of polarizing filters for terrestrial vegetation (Curran 1979). The dynamic range of polarisation measurements markedly reduced with increasing flying height. As Curran equated degree of polarisation with surface roughness the polarisation was seen to be scale dependant. These studies showed the necessity for off-nadir or oblique photography somewhere

[17] Distortions are inherent in all imagery not taken at infinity.

[18] Omega: rotation around the x-axis, phi: rotation around the y-axis, kappa: rotation around the z-axis. For relative orientation x-axis is the direction of flight. For absolute orientation x-axis is 90 degrees clockwise from grid north, or grid east, assuming Transverse Mercator projection.

near the Brewster Angle (Brewster 1815)[19]. This being said, there exists the possibility of polarisation parameters to be used as an adjunct to radiance to help discriminate features inseparable using radiance alone (Chandra and Bothle 2001).

### 2.8.2 Satellite Film Photography

The use of astronaut small-format photography from the early Mercury, Gemini and Apollo missions has been suggested for seagrass mapping (Kelly and Conrad 1969). With the International Space Station's Destiny Lab window[20] there is the opportunity to use this technique today. Digital scans of the photography are available on the internet. However, on inspection, these are of low resolution and suffer from atmospheric scattering and haze. The original film (or at least a copy of the original) can be scanned and analysed at a much greater resolution (Robinson et al. 2002). One study scanned film covering seagrass beds in Shoalwater Bay, Queensland to achieve a ground resolution of 17 metres (Robinson, et al. 2001). This was then used to map seagrass and mangroves. The authors make the point that the advantage of scanned film is the low technology needed (photograph editing versus specific image analysis software ie Adobe Photoshop versus ERDAS Imagine) for planning field surveys. This advantage is doubtful if Landsat, SPOT or ASTER imagery is available.

Historical declassified spy satellite photography has been released to the general public. The United States Corona satellite photography, for instance, was taken using 70mm panchromatic panoramic film from fore and aft cameras, with a nadir ground resolution of around 3 metres (McDonald 1995). Unfortunately for seagrass mapping the film spectral response or filter transparency, on inspection[21], appears to be in the red part of the spectrum. This was probably to minimise atmospheric scatter. The images showed no water penetration.

---

[19] A fuller explanation of the Brewster Angle is presented in section 2.12.

[20] See http://science.nasa.gov/headlines/y2002/29may_lookingglass.htm

[21] Personal inspection of Corona photography over Adelaide (taken 18th November 1966) shows irrigated areas such as school ovals and golf links to be dark due to photosynthetic absorption, and clear water bodies also to be dark. This demonstrates that the film is sensitive to red. Only shallow, low tide areas are visible offshore, as the water column absorbs the red light.

Likewise declassified Russian space photography is available commercially. This is large-format, and so is suitable for film-based analogue or analytical photogrammetry[22].

Overall the use of historical or recent satellite small-format film photography for seagrass mapping is only an adjunct to traditional methods.

### 2.8.3 Satellite Medium Resolution Multispectral Imagery

Medium spatial resolution satellite sensors (~10 – 100 metre ground resolution) such as Landsat and SPOT have been used for seagrass mapping, with varying but usually positive results in localised studies such as individual bays or islands (for example Alberotanza et al. 1999, Maselli et al. 2005, Schweizer et al. 2005). Usually the interpretation is based on the assumption that dark patches are seagrass, though dark substrate, reef and macroalgae can be mistaken for seagrass. Sand however is usually classified correctly (Schweizer et al. 2005).

Thomas et al. (1999), in a review of benthic remote sensing, presents the anecdotal evidence that satellite remote sensing is not useful in Australian waters, evidenced by the small number of papers in the peer-reviewed literature compared to aerial photography. They speculate that this may be due to the lower resolution compared to aerial photography or high-resolution satellite imagery, but one study found that 10 metre SPOT imagery was of a higher accuracy in mapping seagrass than 2.5 metre SPOT imagery (Pasqualini et al. 2005).

Recent studies using Landsat TM and ETM+ bands 1, 2 and 3[23] have mapped both bathymetry and bottom cover (for example Maselli et al. 2005, Schweizer et al. 2005, Dekker et al. 2005). These studies were restricted to depths around five metres due to the use of band 3 (visible red) in the analyses. Misclassification due to band striping is a problem as the signal over water is near the noise level of the sensor system (Maselli et al. 2005).

---

[22] The TK-350 camera has a 10-metre resolution at a scale of 1:630000. The KVR-1000 camera has a 2-metre resolution at a scale of 1:220000. See www.tec.armay.mil/tio/SPIN2.htm accessed 07/12/2005.

[23] Band 1: visible blue (0.45 – 0.52 microns), Band 2: visible green (0.52 – 0.60 microns), Band 3: visible red (0.63 – 0.69 microns).

Seagrass studies are highly dependent on image processing and feature extraction methods. One study using thresholded band ratios detected known dense seagrass beds, but further processing techniques on the same image detected no seagrass beds at all in the study area (Hashim et al. 2001).

### 2.8.4 Satellite High Resolution Panchromatic and Multispectral Imagery

High-resolution satellite sensors have a high dynamic range suitable for low light conditions as found in terrestrial areas of low sun angle, or highly absorptive media such as water. This, however, is wavelength dependent due to atmospheric Rayleigh scattering reducing contrast and radiometric range in the darker digital numbers, particularly in the shorter wavelengths (Mumby and Edwards 2002). This can be corrected using atmospheric and water column modelling to convert the density numbers to albedo (Mishra et al. 2005) or normalisation of images using pseudo-invariant features (Rowlands et al. 2008), or if conditions are clear at time of image capture and the water is shallow (Vela et al. 2008). As with aerial photography sun-glint and wave patterns affect the imagery, but can be corrected for using the near infrared band to map sun-glint intensity and so subtract it from the other bands (Hochberg et al. 2003). The use of the near infrared to correct for surface effects would be applicable to digital aerial imagery.

The main inhibitor for the use of high-resolution satellite imagery is not technical, but the high cost, depending on the size of the study area. For small areas high-resolution satellite imagery is cheaper than flying new photography, especially when aircraft basing charges are taken into account. However the cost of high-resolution satellite imagery rapidly rises until aerial imagery becomes relatively cheaper due to economies of scale in a mature industry. Both methods rely on photointerpretation for analysis (Andréfouët 2008) and so can be treated as datasets that can be interchangeable.

### 2.8.5 Airborne Hyperspectral Imagery

The promise of hyperspectral remote sensing in benthic mapping is the discrimination of seagrasses and macroalgae into taxonomic groups based on their spectral signatures. The main difficulties are calibration of the imagery across and

between flight lines or swaths (Alberotanza et al. 1999), atmospheric effects and the bi-directional reflectance distribution function (BRDF). To correct for these factors involves complex processing, and the end result is a range of benthic information such as water depth (Carmody et al. 2008), location of coral reefs, and detection of macroalgae in shallow waters (Datt et al. 2008, Harvey et al. 2008, Pinnel et al. 2008). Hyperspectal seagrass mapping appears to be more accurate than that using medium and high resolution satellite imagery, but the cost is much higher (Phinn et al. 2008).

Currently hyperspectral remote sensing appears to be still in the research and development stage in regards to marine benthic mapping, needing fuller spectral libraries of benthic communities and types for further development (Blackburn and Dekker 2006).

### 2.8.6 Lidar

Light detection and ranging (Lidar) has been used predominantly for bathymetry, using timed pulses to measure underwater topography, rather than differentiating bottom types. The laser used for bathymetry, unlike terrestrial lidar, has a wavelength normally in the blue-green part of the spectrum. Terrestrial lidar usually operates around 1.0 microns[24], in the near infra-red, which is unsuitable for water penetration due to absorption at this wavelength. Even at around 0.5 microns the laser pulse suffers energy loss due to reflection, scattering and absorption in the water column and the bottom type. It has been estimated that the return signal fades out when the water column is deeper than two to three times the Secchi depth (Smith et al.. 2000), depending on whether the water is dominated by absorption or scattering respectively (Guenther et al. 2000).

The backscatter return signal from the sea floor used for the bathymetric measurement has an amplitude that is the result of the combination of water attenuation and bottom reflectance. Water attenuation is usually exponential, while bottom reflectance is linear (Guenther et al.. 2000). The strength of return signal in clear waters can therefore be related to water depth (actually path length in water), which is known from the pulse timing, and bottom reflectance. As path length (and therefore attenuation) is known, therefore the bottom reflectance should be able to be

[24] Lidar lasers pulse in infra-red at 1.064 microns or in green at 0.532 microns.

related to strength of the return signal once the other factor is removed. That being said, there is little in the way of seagrass or other benthic flora studies using lidar in the published literature, though this is starting to be addressed (Wang and Philpot 2007). This may be due to the bathymetric aspects of the technology dominating the research and development interests. Another reason may be the greater appropriateness of other remote sensing systems such as hyperspectral for characterising bottom type (Smith et al. 2000).

### 2.8.7 Side Scan Sonar

Side scan sonar, being an active acoustic system, is analogous to side-looking radar (Siljeström et al. 1996). In this instrument the active pulse interacts with the material and the structure of the target to generate the return signal. The main use of side scan sonar is for bathymetry, but as with bathymetric lidar there have been few studies specifically for benthic flora mapping. The few studies published in the literature rely on the structural response of seagrass to the sonar signal as different from bare substrate, therefore hard edges (trawl-lines, effects of dragging boat anchors, detonated high explosive craters) are visible in presence-absence classifications. Side scan sonar has been useful in detecting the deep-water edges of seagrass meadows where traditional remote sensing has difficulty (Pasqualini et al. 1998, Pasqualini et al. 2000). With different sonar frequencies two-band datasets can be created for classification, but again only into presence-absence of seagrasses (Siljeström et al. 1996). Both studies suffered from not using original digital data, but scanned hardcopy, and both used relatively small datasets.

### 2.8.8 Underwater Videography

The combination of underwater video camera, differential GPS and GIS have enabled records of transects to be spatially located (Norris et al. 1997). This method is currently used for marine park planning in South Australia, the advantage being that the data is a permanent record and is geocoded, allowing for comparisons to be made over time. The individual video frames can be extracted, geocoded and feature matched to produce mosaic map strips (Gracias and Santos-Victor 2000).

The problem, as with any transect, is that the video records only a belt transect sample of benthic cover. The intervening areas are either interpolated or left as unknown. The coverage of transects can be limited, as the video collection is quite time consuming. The best method would to undertake a comprehensive survey to capture as much as the sea floor as possible (Stevens and Connolly, 2005). That being said the method has been shown to detect changes in seagrass beds even though it is a sampling technique (Schultz 2008). The main advantage if cost is a major factor would be to use it as ground-truth for other image-based remote sensing techniques (McGoldrick and Leach 1998)[25].

### 2.8.9 Airborne Digital Cameras

There is very little literature regarding the use of airborne digital cameras for benthic flora mapping. Terrestrial use is more widespread, especially taking advantage of red/infra-red band combinations for vegetation mapping (Wallace et al. 2008).

Aerial digital cameras come in two broad formats; mounted off-the-shelf small format cameras, which include video frame grabbers, and cameras designed to simulate the geometric properties of large format film aerial cameras (Hinz and Heier 2000, Dare 2004).

The mounting of small format film cameras on aircraft dates from the beginning of aerial photography a century ago and is still used as a low cost alternative to large format cameras for benthic mapping (Long, et al. 1994, Cuevas-Jiménez et al. 2002). Small format cameras can be used photogrammetrically to map shorelines and beach profiles (Hapke and Richmond 2000).

With the recent development of aerial digital cameras there is the option of 4-band imagery, either with standard blue, green, red, and near infra-red, or with specific waveband filters. The radiometric range is greater than scanned film negatives, which gives the possibility of detailed discrimination in low light (low intensity = fewer photons) conditions. Under the right field conditions standard of-the-shelf small format cameras can be used to detect seagrass in deeper waters (Mount 2003).

[25] The South Australian Department for Environment and Heritage uses a four tiered approach for benthic mapping to overcome these limitations. Satellite imagery is used for broad scale mapping, aerial photography for detailed areas, side scan sonar and videography for strip profiles, and diving for field sampling.

Large format digital imagery has made little impact on the literature so far, particularly in Australia. This may be due to the only recent introduction of the technology and the even more recent uptake by Australian commercial aerial imagery providers (Byrne 2005, Tadrowski and Orchard 2005).[26] One advantage related to the GPS/IMU is that traditional aerotriangulation can be extrapolated over water. Whereas earlier rectification methods relied on coastal ground control, meaning only frames with visible land could be rectified, entire blocks of photography over water can now be rectified to terrestrial accuracies (Cameron 2008).

## 2.9 Summary of Previous Benthic Flora Remote Sensing Studies

From this review certain patterns of sensor use for the remote sensing of benthic flora can be discerned. Aerial film photography has been, and continues to be, the sensor of choice, albeit with all the limitations of broad spectral range. Medium resolution satellite imagery has been used, but suffers from low resolution and few usable bands. Astronaut film photography suffers from the low resolution of satellite imagery and the patchy nature of acquisition. Underwater videography is operational but is a sampling technique rather than a full census of benthic cover.

Areas of potential investigation of sensors for the remote sensing of benthic flora include high-resolution satellite imagery, airborne hyperspectral imagery, lidar, side-scan sonar and airborne digital camera imagery. Each of these have attributes that may be useful. High-resolution satellite sensors have a narrow field of view compared to aerial photography which, if nadir viewing, removes refraction effects, as the light rays are normal to the surface. Some high-resolution satellite sensors have bands in the blue and green parts of the spectrum, which allow for good water depth penetration, and band(s) in the infra-red which can be used to remove surface

[26] The aerial photography industry in Australia is currently going through a transition from film to digital. Most Australian state governments capture aerial photography for mapping and monitoring programs. Some states such as Tasmania (in-house) and Western Australia (single commercial company) are film based. New South Wales operates its own digital system (ADS40 line scanner), while other states and Northern Territory outsource to a range of commercial companies operating film and/or digital photographic systems. In South Australia all state government aerial photography for FY 2006/07, and 2007/08 was digital, though not intentionally, as photography procurement is based on request for quotes, with evaluation of quotes on fitness for purpose, value for money and risk. The 2007 Adelaide seagrass mapping used a digital camera (Cameron 2008).

effects such a waves and sun glint. Airborne hyperspectral sensors have narrow wavelength discrimination which may be useful for seagrass/ macroalgae/ substrate classification. Lidar, although used for bathymetry (based on time delay), does have a backscatter radiance component that has been used to create terrestrial images. Whether bathymetric lidar in the visible green returns a useable radiance is yet to be investigated. Side-scan sonar, like lidar, is an active system that does measure strength of return signal, but is poorly investigated for substrate structure. Airborne digital cameras, while designed to be a replacement for film cameras, actually have greater dynamic range than film, and capture blue, green, red and near infra-red concurrently, whereas film is limited to three spectrally sensitive emulsion layers.

Advances in optical sensors are currently centred on improvements in spatial resolution, spectral range and resolution, and dynamic range. There is a lack of development in the use of photon properties other than intensity and wavelength, such as polarisation. A combination of an airborne digital camera with a polarisation filter rotated at a specific angle should increase contrast in turbulent waters, and reduce surface reflection. This is a promising area for remote sensing of marine benthic flora and is the subject of the following section.

## 2.10 Introduction to the Physics of Optical Remote Sensing

Remote sensing of the visible and infra-red (reflective and emissive) parts of the electromagnetic spectrum uses intensity and wavelength as the primary measurable quantities[27]. These two quantities are the basis of all subsequent digital image processing and feature extraction. While strongly empirical, remote sensing has a theoretical basis in classical electromagnetic theories. While the current approach relies on the concept of an electromagnetic wave, other approaches may open new insights. This may lead onto new ways of designing remote sensing experiments and of interpreting the remote sensing signals.

## 2.11 Background Concepts

The traditional approach in remote sensing has been to use the term wavelength for the visible, infra-red and thermal parts of the spectrum, and frequency for the

[27] While secondary measurements, such as direction which is used to define location, intensity and wavelength can be analysed without reference to ground location.

microwave (passive and radar) parts of the spectrum. This is mainly due to history, with wavelength the preferred term in optical astronomy, and frequency the preferred term in microwave sciences such as radio and radar.

Most sciences use theoretical models that are best suited to their particular area of study. There are several conceptual models used in image analysis. For example, photogrammetry, as a geometric science, uses the concept of rays as the theoretical model (Burnside 1979). The concept of rays and central perspective images dates back to the works of Leonardo DaVinci (from 1492 onwards) and mathematically to Johann Heinrich Lambert in 1759. Apart from advances in photography and autocorrelation, photogrammetric theory is still based on geometric ray tracing.

Remote sensing uses the concept of transverse waves of light, having properties of wavelength, frequency and amplitude[28]. The wave theory of light, while dating back to Christiaan Huygens (Gribbin 2002) only became the accepted theory in optics, superseding Isaac Newton's corpuscular theory, in the beginning of the 1800's, when Thomas Young applied mechanical wave equations to optics. Light was later shown by James Clerk Maxwell to be an electromagnetic wave caused by accelerating electrical charges, though optical theory was slow to take on the new concept. With the discovery of the electron by J. J. Thomson a physical basis for Maxwell's equations was demonstrated by Hendrick Lorentz in 1899 (Gribbin 2002).

In the twentieth century problems with classical wave theory of light introduced the concept of quantisation of light, in that light is not a continuous wave but has discrete quantile properties. Quantum electrodynamics theory specifically deals with the interaction of light with matter, or more specifically photons with electrons. In the Feynman approach (Feynman, et al. 1965, Feynman, 1985) photons are treated as particles of light, with wave-like properties of photons an expression of underlying quantum properties such as the wave-particle duality of photons and particles (Copenhagen interpretation, Gribbin 2002).

Photons have a range of properties. The properties most measured in remote sensing are intensity (number of photons per unit time and unit area) and the paired property of frequency/ wavelength. At the level of a single photon wavelength is

[28] Wavelength being the distance between the wave crests (or any other part of the wave that cyclically repeats), frequency being the number of wave crests passing a point in a certain time, and amplitude is related to the energy of the wave, in that the square of the amplitude is the intensity of the wave.

equivalent to frequency, which is equivalent to energy in joules, which is equivalent to energy in electron-volts (Lehrman and Swartz 1969). Therefore photon-electron interactions can be modelled in any of these measurement systems. For example, using photon energies may better represent florescence and photosynthesis, as both processes take photons of certain energies and convert to lower energies (Collett 1993). The advantage of reformulating in terms of electron-volts is that photosynthesis research is based on the transport of electrons at quantum energy levels (Fong 1982), and so meshes with current photosynthesis models (for example Ralph and Gademann 2005).

An individual photon has, as well as wavelength/frequency, related properties such as energy, momentum and angular momentum[29]. Intensity is, unlike wave theory, a measure of the number of photons, rather than a property of an individual photon. Likewise amplitude (actually the square of the amplitude) is a measure of the probability of finding a photon at a particular location rather than transverse displacement by a wave (Feynman 1985).

## 2.12 Polarisation

Polarisation is a largely ignored third property of light, after amplitude and wavelength. This property has been little utilized in remote sensing (Egan 1985). This may be due to the geometric nature of polarisation measurements, in that the light source – target – sensor angle has a major contribution to the final value. Most remote sensing studies have been in relation to terrestrial vegetation (Curran 1978, Curran 1979, Curran 1981) and polarisation has been recognised as an adjunct measurement to separate features indistinguishable by radiance alone (Chandra and Bothle 2001). Ground polarisation images of desert pavements have shown intensity and colour variations due to polarisation of reflected light (Hibbitts and Gillespie 2008).

Polarisation, as a concept, has been explained by several models. These models, while having narrative strengths, tend to push analogy beyond observed phenomena. An example is the picket fence analogy, where only polarised light aligned to the vertical gaps in the fence are let through, and all the rest blocked. Measurements

[29] Electromagnetic wavelength ($\lambda$) and frequency (f) are related through the speed of light (c) via $\lambda = c / f$. Energy (E) is related to frequency through Planck's constant (h) via $E = h f$. Momentum (p) is related to wavelength also through Planck's constant via $p = h / \lambda$.

show that light polarised at an angle to the vertical gaps can 'get through' in some proportion, with only linear polarised light at 90 degrees to the picket fence gaps are totally blocked. Most mathematical models of polarisation depend on either a classical physics or quantum-mechanical approach. Stokes (1852)[30] developed a mathematical description based on observed phenomena that conformed to both classical wave physics and quantum physics (Collett 1993)[31]. Four measurements (vertical polarisation, horizontal polarisation, polarisation at 45 degrees, and intensity) are sufficient to define the Stokes polarisation parameters. These parameters define the state of the polarisation, that is, whether the light is (1) unpolarised, (2) partially polarised, or (3) elliptically polarised. Elliptically polarised light can be either linearly vertically or horizontally polarised, linear +45 degrees or -45 degrees, or right or left circularly polarised.

The experimental design for this research was based on the Stokes Polarisation Parameters. In classical physics these parameters define intensity, amount and shape of polarisation. In quantum physics they define the number of photons, the orthogonal polarisation states for a photon, and the relative probability of a photon to pass through an analyser at a particular orientation. As such they are applicable in both classical and quantum formulations. The four parameters are *I, Q, U* and *V*, where $I$ is the intensity (number of photons), *Q* is the difference in the amount of polarisation in two perpendicular directions (say horizontal versus vertical), *U* is the difference in the amount of polarisation at 45 degrees to the original orientation *Q, and V* is the amount of circularly polarized radiation

Though normally treated as matrices, these are traditionally termed vectors, ie:

$$I = \langle A_x^2 + A_y^2 \rangle = A^2 ,$$

$$Q = \langle A_x^2 - A_y^2 \rangle ,$$

$$U = \langle 2A_xA_y \cos\gamma \rangle ,$$

$$V = \langle 2A_xA_y \sin\gamma \rangle .$$

[30] Interestingly this paper also reports on the spectral properties of red macroalgae (Rhodophyceae), amongst other substances.

[31] George Gabriel Stokes introduced the parameters in papers published in 1852. These were little recognised until re-introduced in the 1940s (Collett 1993, pp405-6).

Where $A_x$ , $A_y$ are amplitudes of photons in mutually perpendicular directions, $A^2$ is the intensity, $\gamma$ is the phase angle between $A_x$ and $A_y$, $< >$ indicates time averaging, and $I^2 = Q^2 + U^2 + V^2$.

So to get a complete description the following needs to be measured: intensity (ie light intensity), vertical polarisation (0 – 180 degrees), horizontal polarisation (90 – 270 degrees), and the polarisation value at 45 degrees

This can be done in practical terms by using three sensors, each with a polarisation filter at appropriate angles. Intensity ($I$) can be measured directly with no polarisation filter

Sunlight on entering the water surface at the Brewster Angle (53 degrees) is separated into horizontally-polarized reflected photons (noise) and vertically-polarized refracted photons which after absorption and reflectance becomes the return signal. The Brewster angle ($\theta_p$) is found by: $\theta_p = \tan^{-1} (n_2/n_1)$ where $n_2$ is refractive index of water and $n_1$ is the refractive index of air (Pedrotti and Pedrotti 1993), therefore $\theta_p = \tan^{-1} (1.33/1.00) \sim 53$ degrees from zenith (Slater 1980).

As well volume scatter in water is polarized by turbidity particles. By measuring only vertically polarized light the signal can be separated from the noise i.e. the Stokes $Q$ parameter.

Based on the Stokes $Q$ parameter there should be an increase in contrast between dark and light areas in an image if the contribution of surface reflectance and volume scatter can be eliminated.

## 2.13 Other Factors Influencing the Absorption and Polarisation of Photons in the Remote Sensing of Marine Benthic Flora

### 2.13.1 Reflection and Refraction at the Air/Water Interface

Refrangible[32] photons when going from one medium to another, such as air to water, experience a change in velocity (speed, direction, momentum) that is different for different energies (wavelengths). Note that the frequency of light going between different media does not change. This change results in a refraction of photons towards the normal when going from a less dense to a denser medium, and *vice versa*.

With dielectric[33] media such as water, the degree of polarisation of the reflected light is dependent on the angle of incidence and reflection. At a certain angle (Brewster angle) the reflected light is solely horizontally polarized, whereas the refracted light has both horizontal polarisation and other polarisation properties (Brewster 1814, Brewster 1815, Brewster 1830a, Brewster 1830b). This means that a vertically polarized analyser can completely filter out the partial reflection of incident light (usually around 16% (Feynman 1985)).

### 2.13.2 Absorption by Water

Light absorption by water is exponential with depth and is wavelength dependent. Lambert's law expresses this relationship[34]. Derived empirically, $I_z = I_o e^{-\mu z}$ where $I_z$ is intensity at depth, $I_o$ is surface intensity, $\mu$ is the extinction coefficient for a particular wavelength, and z is the depth (Slater 1980). Absorption in water reaches a minimum at around 0.48 microns (blue-green) and so this is the optimum wavelength for underwater imaging. The high absorption in the near infra-red means that any signal received by the sensor at these wavelengths is pure surface reflection.

[32] Capable of being refracted.

[33] Material which resists the flow of electricity.

[34] Extinction coefficients can be found at http://www.lander.edu/RSFOX/415lightLec.html accessed 19/04/2006.

### 2.13.3 Scattering in Water

Scattering, in terms of remote sensing, has the effect of reducing the contrast between target and background (Egan, 1985). The increase in background brightness is directly proportional to the amount of scattering. When scattering increases, say due to turbidity, then the contrast, in the example of seagrass and sand, approaches zero. This means that, unlike absorption, increases in source intensity (brighter light) or increases in sensor efficiency (the ability to detect fewer photons, or better signal to noise ratio) will not result in any increase in contrast.

However, empirical measurements have found that using a circular polarisation analyser contrast improvements of a factor of 5-20 have been achieved in turbid media (Egan, 1985, Gilbert and Pernicka 1967). This is generally explained by there being only a single scattering event by turbidity particles, resulting in opposite circular polarisation to incident photons, whereas the target scatters multiple times and so has equal polarisation handedness. By removing the photons due to scattering by turbidity particles by using a circular polarisation filter, the target contrast is improved[35].

## 2.14 Photosynthesis

Current models of photosynthesis are based on quantum electrodynamics, in which photons of light with certain energies release electrons from chlorophyll molecules, which is then eventually used to create carbohydrates. Energy is fed from antenna chlorophyll molecules that capture photons with higher energy, to the active chlorophyll molecule at a lower energy.

Due to the high extinction coefficient ($\mu$) in the red part of the spectrum, photosynthesis using low energy photons is not possible at depth. Seagrasses have evolved to maximise the efficient use of higher energy photons in the blue part of the spectrum. The amount of energy available is directly related to the number of quanta available for photosynthesis (Morel and Smith, 1974). However if the photosynthetic molecules are not attached to accepter molecules then the energy is released as fluorescence (Seddon and Cheshire 2001).

[35] Several marine predators use polarisation vision to detect prey at low target/ contrast ratios (eg Shashar and Cronin 1995, Shashar *et al.* 2000, Parker 2003)

## 2.15 Scattering and Absorption by Substrate

Not only the spectral response of benthic flora needs to be considered but also the spectral response of the 'background', the substrate (Maritorena et al. 1994). This can be of several kinds in the South Australian marine photic environment: ie rock, quartz sand, calcareous sand, and seagrass matte (Shepherd and Sprigg 1976).

Quartz sand, usually of terrestrial origin, underlies the seagrass meadows both off the Adelaide metropolitan beaches and off Yorke Peninsula in Gulf St Vincent. The rest of the gulf is calcareous, mainly of biological origin. This substrate consists of reworked remains such as from the destruction of molluscs in shallow, high wave energy waters, and of bryozoa, calcareous algae and foraminifera in deeper waters (Shepherd and Sprigg 1976). Rocks with sessile macroalgae are found as reefs and around rocky headlands.

Wet quartz sand has a lower reflectance than dry, 18% compared to 42% (Kühl and Jørgensen 1994). This is due to the smaller difference in refractive index between quartz and water than between quartz and air. This results in a higher forward scatter into the sand, and resultant longer path length (or time within the sand), leading to a higher probability of multiple scattering by electrons and higher probability of absorption. Absorption is dependent on wavelength, with shorter wavelengths (~0.45 μm) penetrating shorter distance into the sand before being absorbed (Kühl and Jørgensen 1994). Though of reduced contrast, this backscatter is still high compared to that of benthic flora. This is confirmed by the contrast between sand and seagrass on aerial photography, and the brightness of dry beach sand.

Marine sediments, consisting of quartz and calcareous sand grains, diatoms and amorphous organic material, have a similar spectral response to wet quartz, however are modified by absorption by chlorophyll *a* at around 0.675 μm (Kühl and Jørgensen 1994). Although the red part of the spectrum is not used for remote sensing of marine benthic features due to water absorption, the extra absorption by chlorophyll in such sediments *a* would cause reduced contrast between substrate and flora.

## 2.16 Image Quality

### 2.16.1 Introduction

There is no current universally recognised single measure of image quality (Luo, 2006). There exists a range of measures or indicators of image quality, such as contrast, signal-to-noise, sharpness, resolution, point spread function (PSF) and modulation transfer function (MTF), each of which can give indications of image quality.

These indicators or measures are indicative of the entire image capture system and environmental conditions at time of image capture. The final quality of the resultant image relies on the ambient light source, atmospheric and (for seagrass) marine conditions, lens quality, camera, shutter speed, image chip, data format and data compression.

In operational aerial photography projects assessment of image quality has been largely subjective. This can be quantified to a certain extent using the concept of fitness-for-purpose. Here the quality is defined by ground features in the image being visible or not visible. Four types of ground features are considered – high contrast linear, low contrast linear, high contrast area and low contrast area. Depending on feature visibility or not, the image is rated on a scale loosely related to ground sampling distance. This method is a simple application of the modulation transfer function and ground sampling distance as an operational single value measure. The number rating can then be indicative of what purpose the imagery is fit for.

### 2.16.2 Resolution

The resolution of traditional film photography is measured in line pairs per millimetre at a certain contrast ratio, usually 1:1000. Specially drawn targets with line pairs of different thickness/ spacing and orthogonal orientation are used, either in a laboratory environment, or on the ground while an aircraft flies over and captures the photography.

Resolution within a single frame aerial photograph varies due to distance from centre of the lens (usually resolution decreases towards the edges) and forward motion of the aircraft (blurring in direction of flight); the amount of forward blurring is a function of aircraft speed, shutter speed and flying height.

Resolution on a survey of aerial photography varies due to a variety of factors. These include shutter speed (itself a function of light conditions and film type), camera and lens quality and stability, film type (traditionally panchromatic film was designed to have a higher resolution than colour film), film processing, air column (scattering being a function of distance and wavelength) and environmental conditions (smoke, haze, condensation, sea spray) at the time of image capture.

### 2.16.3 Modulation Transfer Function (MTF)

The modulation transfer function of a camera system measures the resolution at different contrasts, and is usually presented in graphical form of line-pair resolution (or frequency) versus contrast. The frequency response of a camera system is related to the resolution, in that above certain frequency/ contrast ratios there is a cut-off frequency above which there is no signal (Schowengerdt 2007). The MTF was recommended in 1959 as the recommended image quality measurement of aerial photographic systems (Burnside 1979).

# 3 Pilot imagery experiment

## 3.1 Introduction

This chapter contains the experiment design, summary of results, discussion and conclusions of a pilot data capture mission. The rationale for the pilot data capture flight was to perform a test run to ascertain if there were any unexpected problems with the experimental design. The capture of blue, green, red and infra-red bands was to test whether the polarisation effects were similar across wavelengths from blue to near infra-red. The test data was used to decide whether quantitative image analysis or photointerpretation would be the best approach to analyse the imagery (Richards 1989). The results had a direct influence on the later modified experimental design detailed in the next chapter.

## 3.2 Methods

### 3.2.1 Initial Conceptual Experiment Design

The experiment called for an aircraft mounted digital camera that meets the following criteria: multispectral sensitivity, specifically a blue and/or green band and possibly an infra-red band, rotatable polarisation filter, tiltable camera mounting, and a Global Positioning System (GPS) link

The selection of the green band is due to the low amount of water absorption at these wavelengths. Blue, while having low relative absorption, tends to be subject to more scattering effects than green and which traditionally results in a lower signal to noise ratio, but still gives good water penetration. Infra-red, because of the high absorption in water, returns little to no signal from the sea floor, and so the signal can be used as a measure of straight surface reflectance. The red band contains little useable information over deeper water due to absorption, but what little signal there is can be confused with surface reflectance, and so infra-red was deemed more suitable for imaging pure surface reflectance.


**Figure 1 Initial conceptual design of camera mounted in aircraft camera port.**

A polarisation filter would be rotated to align with the vertical electric-vector, so as to remove horizontally polarized photons.

An adjustable tilted camera mount would be used to capture off-nadir imagery overlapping the Brewster Angle of 53 degrees (figure 1). This would be in the up or down sun direction[36], as polarisation has been found to be ineffective at 90 degrees to the sun direction (Lee et al. 1997).

There are several approaches to determine the six photogrammetric parameters which describe image geometry. The location in space (X, Y, Z) and direction of principal point (omega, phi, kappa) define the absolute orientation of a central perspective image. If using a wide angle field of view, a high oblique image could be used to measure variations in the camera angle due to aircraft pitch (phi, or rotation around the y-axis) and roll (omega, or rotation around the x-axis or direction of flight). The horizon on the image, assuming absence of land, could be used to measure these variations, in the absence of an inertial measurement unit (IMU). A GPS would give the location of the camera (once reduced from the antenna) in X, Y, Z space, or easting, northing and height. This will give the location of each image frame, but not its orientation. The one missing parameter would be yaw (kappa, or rotation around the z-axis). Even though direction of flight can be found using the GPS measurements, the amount of crabbing of the aircraft to keep on track is an unknown. A solution would be a second GPS on the aircraft of known distance and direction from the first GPS, say on the tail or wing-tip. The difference in coordinates adjusted for any off-sets would give the pointing direction of the aircraft and camera.

[36] Up sun: flying into the direction of the sun, eg north at local noon. Down sun: flying directly away from the direction of the sun, for example south at local noon.

This option unfortunately was not possible with the experimental set-up used for the project.

An alternative was to use aerotriangulation to bridge between known ground control points. However there needs to be a correction for water/air refraction across each frame. This would work best with near-nadir viewing imagery rather than high oblique imagery. The camera would need to encompass the Brewster angle with a wide-angle lens as well as nadir. The Brewster angle would need to be derived on each frame from the orientation parameters derived from the aerotriangulation.

Lens distortion of small format cameras is usually an unknown, which for photogrammetric processing would need to be measured and modelled. One option was to image a grid of known coordinates. Another was to image the ground with features of known location and height. These can be used to show any barrel or pin-cushion distortions. The best solution is to calibrate the lens/camera combination.

The absolute positional accuracy of features visible on the imagery depends on a variety of factors, such as non-differential GPS accuracy, measurement precision, refraction, image clarity, lens/ camera distortions, to list just a few. For this experiment, the absolute positional accuracy needed only to be approximate for comparison with other spatially located data sets. The experiments can be spatially indeterminate, so long as the relative factors are accounted for. Therefore no photogrammetric processing was necessary.

### 3.2.2 Initial Operational Methodology

Design of optimum image acquisition methods was based on the pilot imagery flights. Image data capture was planned for in the November-January period, due to the optimum conditions of high sun angles and wider temporal windows (early morning and late afternoon) giving a greater radiometric dynamic range, shorter chip integration time[37], and opportunities for image data capture. This time of year is usually cloud and storm free. Ideally image capture should occur a fortnight or later than any large rainfall events, to reduce river outfall turbidity. Study location options

[37] Polarisation filters generally cause a loss of 1 to 2 f-stops, which means longer chip integration times. This can result in blurring of the image in direction of flight due to aircraft motion if the integration time is too long. This is similar to having a low shutter speed on film-based cameras.

include areas of known seagrass, such as seawards of northern and southern metropolitan Adelaide beaches. These areas have sufficient coverage of other aerial and ground data for flight line design over areas of known seagrass, and for identification of seagrass and substrate on the test imagery.

The experimental design needed to minimise any differences due to environmental conditions, such as time of day, weather and sea surface conditions (Mount 2003).

### 3.2.3 Experiment Design

A pair of co-mounted commercial off-the-shelf cameras was chosen as the basic experimental design. One camera had a standard natural-colour CMOS chip. The other otherwise identical camera had an infra-red filter mounted on the CMOS chip. While the natural colour and infra-red bands of the two cameras would not be exactly co-aligned, the two sets of co-temporal images would be of the same approximate ground locations.

A pair of Canon EOS 350D 3-band digital cameras was chosen for the experiment (figure 2). These have single RGB-sensitive CMOS chips with a raw image size of 3456 by 2304 pixels and a pixel size of 0.0064mm (Canon 2007). One camera had the standard red, green and blue bands produced by a Bayer pattern mosaic of red, green and blue filters over the chip (see below). The other camera has an inbuilt near infra-red filter over the chip, as the CMOS chip is sensitive to the near infra-red.

**Figure 2 Canon EOS 350D camera.**

The cameras both had Canon EF-S 18-55mm f3.5-5.6 II lenses with the filters forward mounted of the lens. Each filter was a 58mm Hoya Pro1 Digital PL (circular polarisation) and were orientated vertically (external frame of reference) on both cameras once mounted in the aircraft.

### 3.2.4 Camera Mounting

The two cameras were mounted in a specially constructed aluminium camera bracket. The cameras were placed upside down relative to each other to fit within the bracket. The cameras nominally pointed 30 degrees forward of nadir. The resultant orientation was portrait. This orientation gave a large amount of forward overlap between adjacent frames. This had the added benefit of giving a field of view from near nadir up to the Brewster angle[38].

The bracket was mounted in the camera port of the aircraft. A translucent Perspex cover covered part of the port to provide protection from engine oil and engine exhaust (figures 3, 4 and 5).


**Figure 3 Aircraft VH-PJE used in pilot data capture. Note the engine exhaust cowling on the forward underside.**

[38] Later measurements showed that the field of view was just over 45 degrees, giving a nominal range from 7.5 degrees forward from nadir to 52.5 degrees forward from nadir in straight and level flight. However the pitch of the aircraft is dependent on speed and trim, so that the actual central angle and the range ends varied during flight.


**Figure 4 Camera port with Perspex cover, external view.**


**Figure 5 Camera port with mounting bracket attached, internal view.**

### 3.2.5 Study Region

The selected region for this pilot study was seawards of the coastline from north of Port Noarlunga South, to south of Sellicks Beach, on the eastern side of Gulf St Vincent, South Australia. This region was selected as having a range of macroalgae and seagrass types, sandy and rocky marine substrates, containing a variety of known landscape and seascape types (Shepherd and Sprigg 1976). This region contains several rocky promontories and sandy beaches, as well as a mixed suburban and rural landscape. The main seagrass type is *Posidonia coriacea*, a seagrass with a distinctive clumping habit rather than the extensive meadows of *Posidonia australis/ Amphibolis antartica* found further north along the Adelaide metropolitan beaches[39].

[39] *Pers comm*. David Miller, Department for Environment and Heritage, and also visible on DEH orthorectified aerial photography.

### 3.2.6 Data Capture

Airborne data capture took place on Saturday 26 November 2006, between 9:30am and 10:24am Australian Central Daylight Time (GMT +10hr 30min). Six post-mounting test images from each camera were captured in the hangar at 8:32 to 8:33am to test the set-up. A single test image from each camera was captured prior to take off at 8:59am.

The aircraft proceeded from Murray Bridge airport directly to the test site. Several short east-west runs were captured in the Seaford-Moana region, and then longer north-south runs between the mouth of the Onkaparinga River and Sellicks Beach (figure 6). The camera continued to operate during aircraft turns. Non-differential GPS coordinates of the aircraft were recorded at time of each image-pair capture.

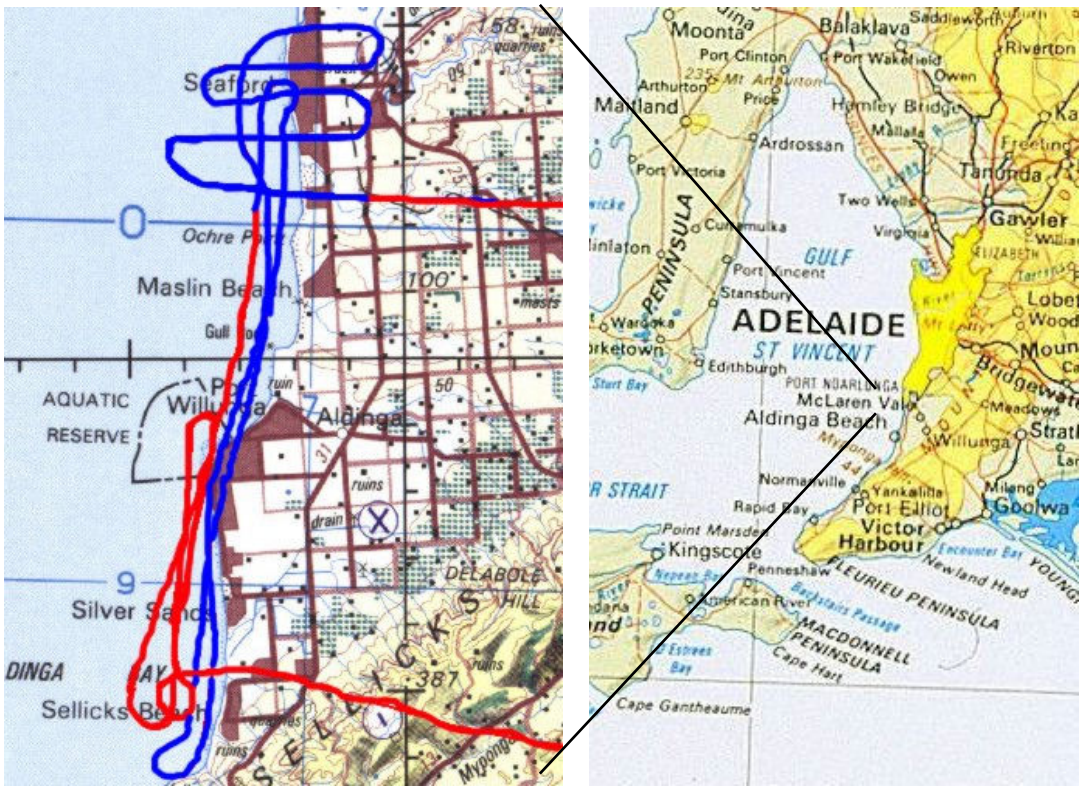


**Figure 6 Flight lines. Blue indicates flight path of data capture. Red indicates flight path with no data capture. Track from Murray Bridge in the north, and track back to Murray Bridge in the south. 1:250,000/ 1:2,500,000 base maps courtesy Geoscience Australia.**

### 3.2.7 Data Supply

The natural colour images were supplied as separate red, green and blue files in TIFF format, plus 3-band thumbnail images in JPEG format. The infra-red images were supplied as a single band file in TIFF format, plus 3-band thumbnail images in

JPEG format. There were 570 visible and 570 infra-red data frames captured, excluding test frames.

The GPS coordinates were supplied in latitude and longitude in decimal degrees, and height in metres. These were converted to Transverse Mercator zone 54 projection in Map Grid of Australia (MGA) coordinates, Geodetic Datum of Australia 1994 (GDA94) using Department for Environment and Heritage in-house DIGMAP software. The height data was in Australian Height Datum (AHD).

### 3.2.8 Image Analyses

As Richards (1986) points out, there are two main approaches to image interpretation: quantitative analysis and photointerpretation. The pilot study aimed to assess the quality of the image data, and decide on the most suitable method for interpretation.

The scale of the photography was determined by measuring ground features on selected images. As the photographs were oblique, the scale and resolution varied from top to bottom on the images. The relative scale was determined by measuring the same ground feature at top and bottom. The absolute resolution was determined by measuring a feature of known size.

Due to the variable nature of the amount of polarisation at each pixel on the images, local rather than whole frame analysis techniques were used. Current whole frame methods were inappropriate as they relied on global statistics.

Two new methods of image analysis were developed for this project. One, termed the profile method, was developed to help visualise noise and vignetting effects, and its subsequent removal using a profile line. This was developed due to the large amount of noise in the data and the off-centre fall-off in density number values in the image over water, making global statistics meaningless. The method was to draw a profile line across the image over a featureless region, such as deep water, the resultant digital numbers along the profile illustrating the shape and amount of vignetting, and the amplitude of the small scale variation demonstrating the noise.

The second new method was to compare contrast of the same seagrass/substrate features at different row values on overlapping imagery. This method was developed

to compare differing polarisation effects on the density numbers from top to bottom of the images. The same feature from overlapping images was excised, the histograms compared, and the resulting range compared. To check that the method was comparing contrast and not some other factor, the same high resolution feature was spatially degraded to the resolution of the lower resolution feature and compared. Bilinear resampling was used to degrade the higher resolution feature, as nearest neighbour would still have a sub-set of the original range of pixel values, whereas bilinear would generate new digital numbers based on the original values.

ERMapper 7.1 (now Leica) software was used for image analysis.

## 3.3 Results

The results from each camera are presented below. The infra-red camera results are presented qualitatively in comparison to the natural colour imagery. The natural colour results are treated more in-depth as these results are equally applicable to both cameras.

Selected frames are used to illustrate points. These frames are representative of tens or hundreds of similar frames. Other frames could also have been selected to illustrate the same effect with no change in results.

### 3.3.1 Infra-Red Camera

Infra-red vertically polarised imagery was captured by a single camera. As there was extremely high correlation between the three bands due to the same filter embedded on the CMOS chip, only a single band was used for the analysis[40].

It was obvious on visual inspection that there was no detail in the images captured over the water. Only surface features such as boats and breaking waves were apparent (figure 7).

Stretching of the histogram revealed only artefacts such as vignetting, noise and internal camera reflections. No detail was visible in the water compared to the natural colour imagery (figure 8).

[40] Interestingly the 3-band thumbnails did show subtle colours of blues and browns rather than the expected greys. Why this was so was not explored as it was deemed outside of the scope of this project.

To test the water penetration properties of the infra-red images further, co-temporal images captured over Aldinga Reef Aquatic Reserve[41] (figure 9) were compared in natural colour and infra-red (figure 10).

The results showed some detail in water depths much less than 1 metre, in the inter-tidal zone. However at permanent seagrass water depths there was no measurable signal. Previous inspection of the area showed the reef to be nearly level, with only a slight slope at the edges of the reef (figure 11 and 12).

The polarisation filters on both the RGB camera and the infra-red camera gave similar results in terms of surface reflectance. Direct sunglare appeared identical on co-temporal images (figure 13). This shows that the polarisation results for the visible bands also apply to the infra-red band.

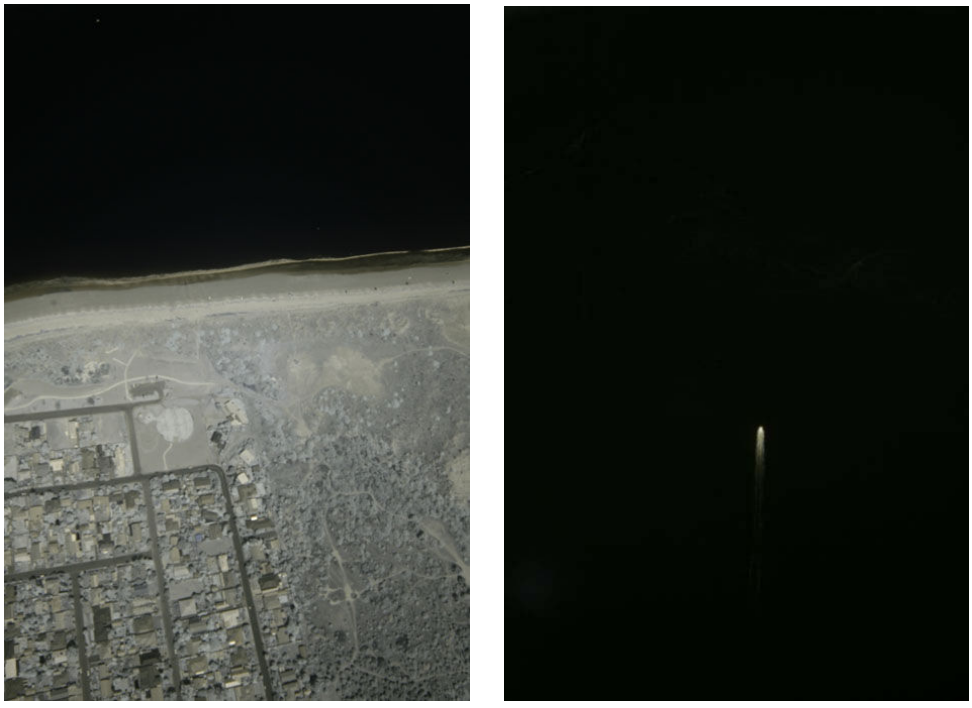

**Figure 7 Thumbnail images showing breaking waves (frame 6194 left) and boat with wake (frame 6435 right). Notice the lack of detail in the water.**

[41] Aldinga Reef Aquatic Reserve comprises a shallow rocky intertidal platform, plus a drop to a subtidal sand and reef complex. Pictures of the reef and its ecology can be found in the plate section of Womersley (1984).

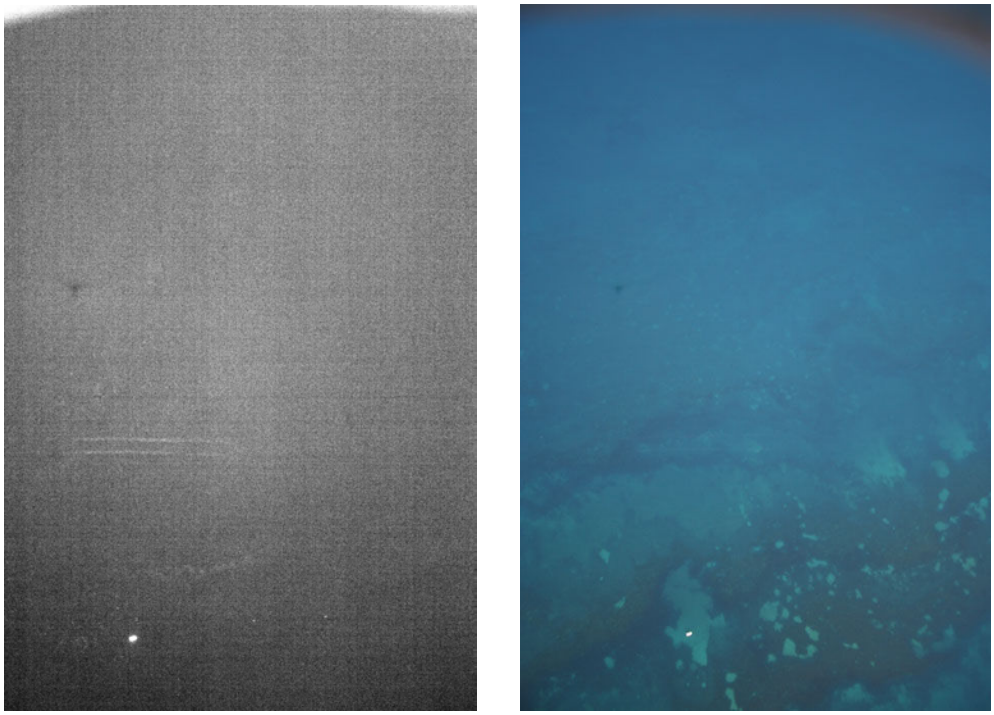

**Figure 8 Infra-red single-band frame 6205 (left) linearly stretched and showing mainly noise, and co-temporal natural colour frame 2078 (right) for comparison. The white dot on both images is a boat.**

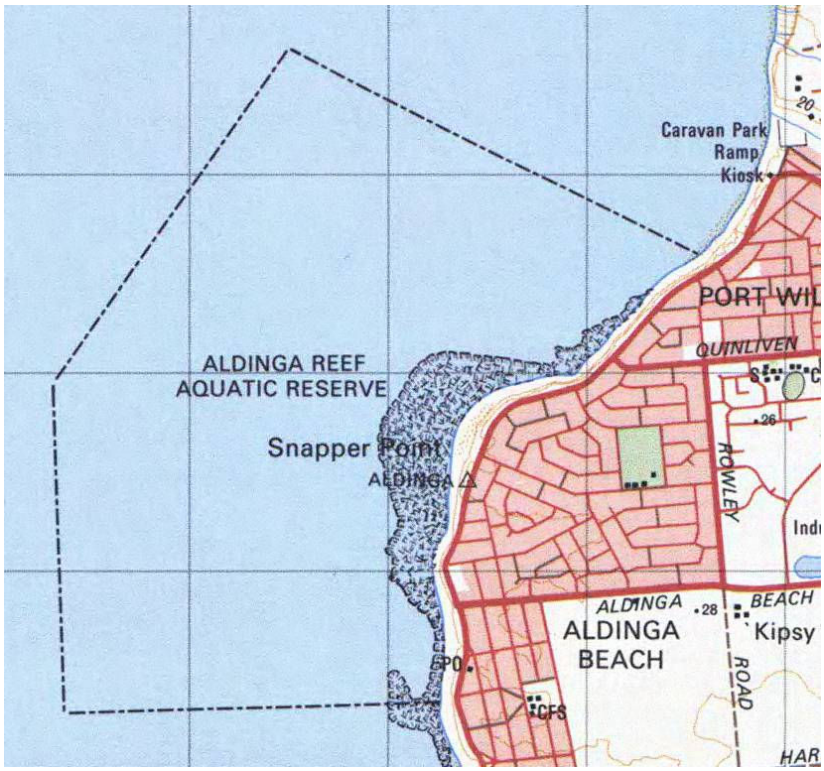


**Figure 9 Segment of 1:50,000 topographic map (courtesy Department for Environment and Heritage) showing the extent of the intertidal reef.**

**Figure 10 Co-temporal infra-red and natural colour images of Aldinga Reef. Water is over the reef. Note the lack of detail in the deeper water on the infra-red image. (Images rotated 180 degrees to bring north approximately to the top).**


**Figure 11 Aldinga Reef as seen from Snapper Point (looking west). The intertidal reef extends from the beach to the breaking waves.**

**Figure 12 Snapper Point as seen from Aldinga Reef (looking east) showing the shallow water coverage at one hour before high tide.**

**Figure 13 Direct sunglare on eastward facing images 6243 (left) and 2116 (right).**

### 3.3.2 Natural Colour Camera

The natural colour vertically polarised imagery was captured by a single camera. Initial inspection of the imagery showed little differentiation of benthic features in images over the water. Also visible were artefacts due to partial masking by the camera port Perspex cover, as well as mobile oil drops on the lens filter (figure 14).

However with balancing, smoothing and linear stretching of the three bands much more detail could be made out on the benthic seafloor. Visually the green band contained the most detail and contrast (figure 15). Stretches on the blue and red bands were of less use in showing benthic detail (figure 16). Concentrating on the green band, what appeared to be subtle shading was revealed as complex benthic patterns (figure 17). Benthic features were clearly visible in the imagery once enhanced, showing that the natural colour vertically polarised imagery had good water penetration.

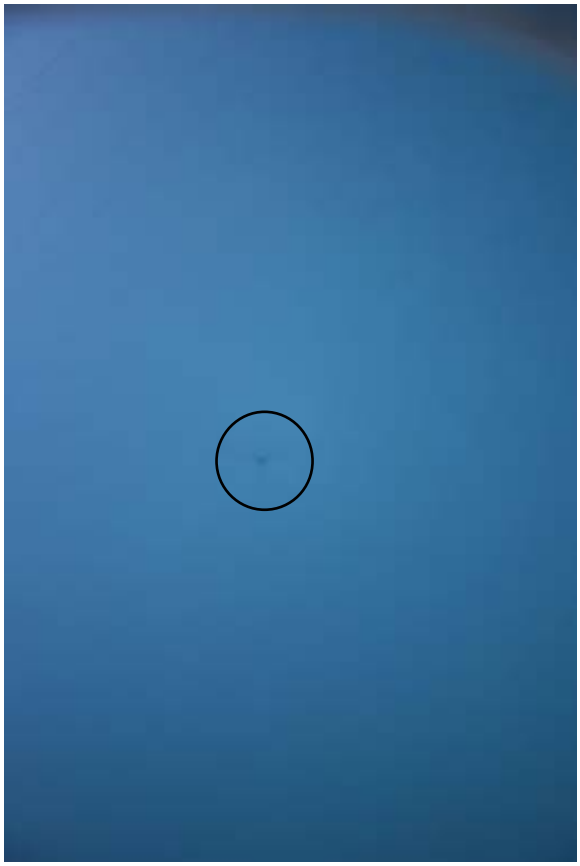

**Figure 14 Frame 2092 showing masking by Perspex cover at top, especially the right hand corner, and oil drop left of centre (circled).**

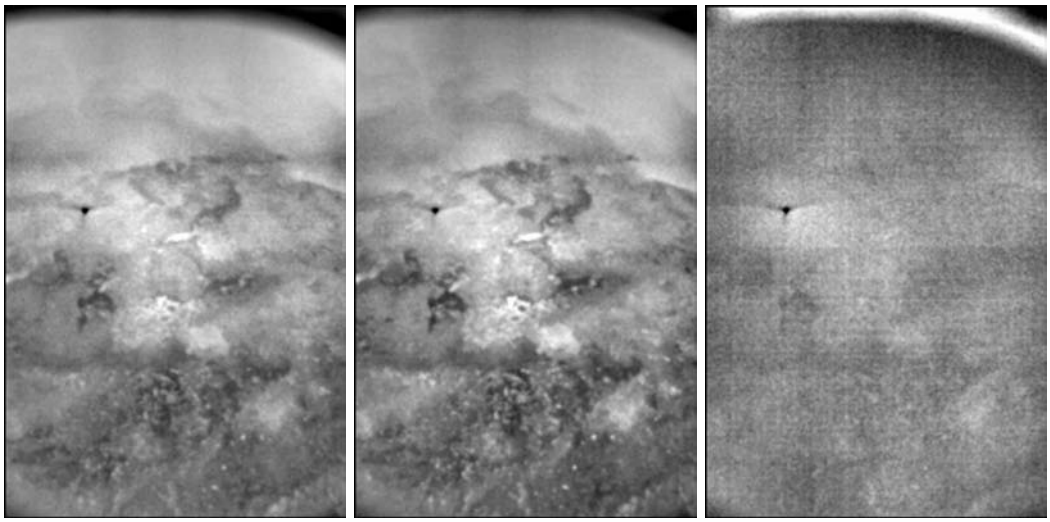

**Figure 15 Frame 2083 blue (left), green (centre) and red bands (right) balanced, smoothed (11 by 11 filter) and linear stretched.**

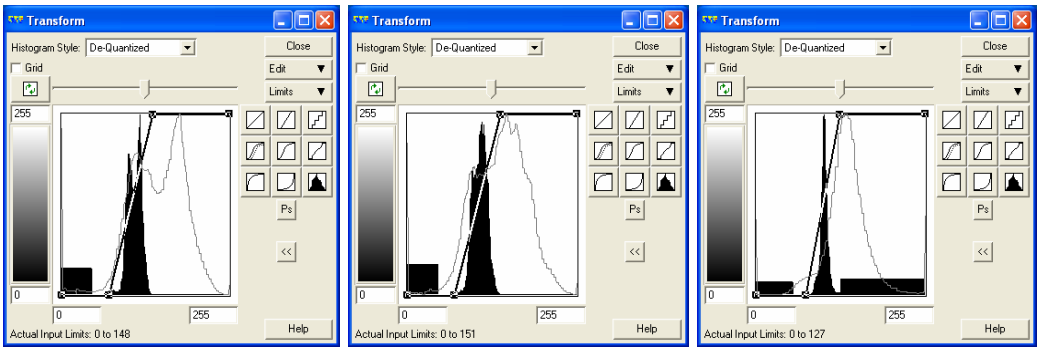


**Figure 16 Histograms of the images shown in figure 15. Blue (left), green (centre) and red (right).**

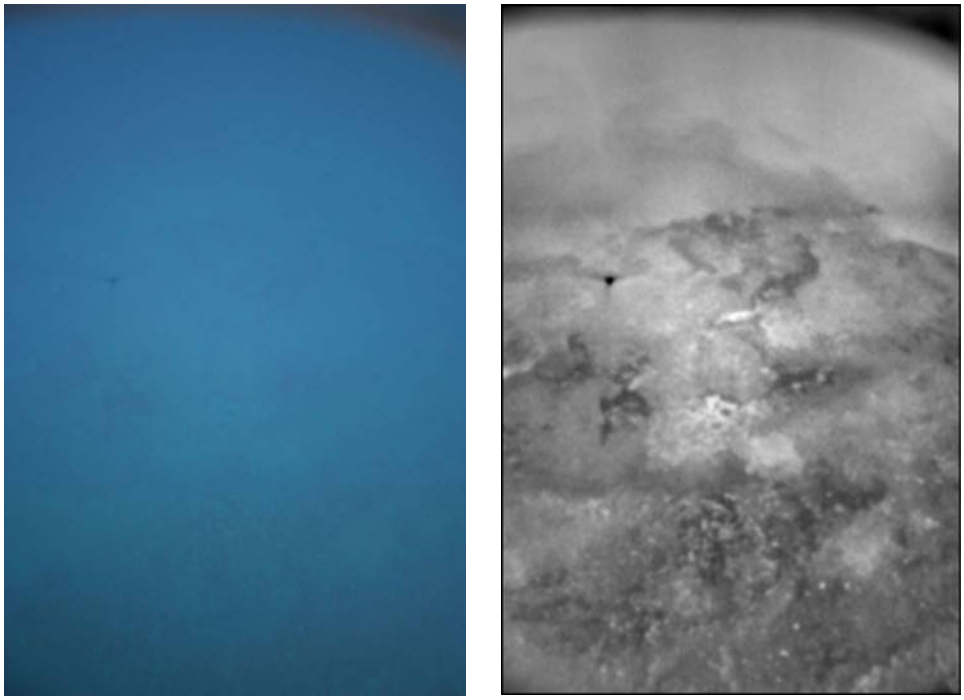

**Figure 17 Direct comparison of frame 2083 showing unmodified natural colour (left) and balanced, smoothed and stretched green band (right) showing benthic detail.**

### 3.3.3 General Observations

The 30 degree forward from nadir orientation, plus the 45.45 degree field of view (top of frame to bottom), resulted in the same ground feature being imaged up to ten times on adjacent frames as the aircraft flew over. The first sighting of any particular feature would be at the top of the frame, near the Brewster angle. The final sighting would be just forward of nadir.

While the nominal angle forward was 30 degrees from nadir, measurements taken on frame 2200[42] showed that the camera was pointing 38.57 degrees forward of nadir.

[42] The aircraft height above sea level and easting were known from the GPS. The aircraft was traveling east so that the northing could be ignored for the calculation. The aircraft height above ground level was the sea level height minus the ground elevation from a DEH 1:50,000

This resulted in the bottom of frame to be 15.84 degrees forward from nadir, and the top of frame being 61.3 degrees forward from nadir. The Brewster angle was calculated to be at line 311 from the top of the image, assuming no aircraft roll.

### 3.3.4 Scale

Due to the change of angle across the image, the scale and resolution changed from top to bottom. The perspective also changed (figure 18).

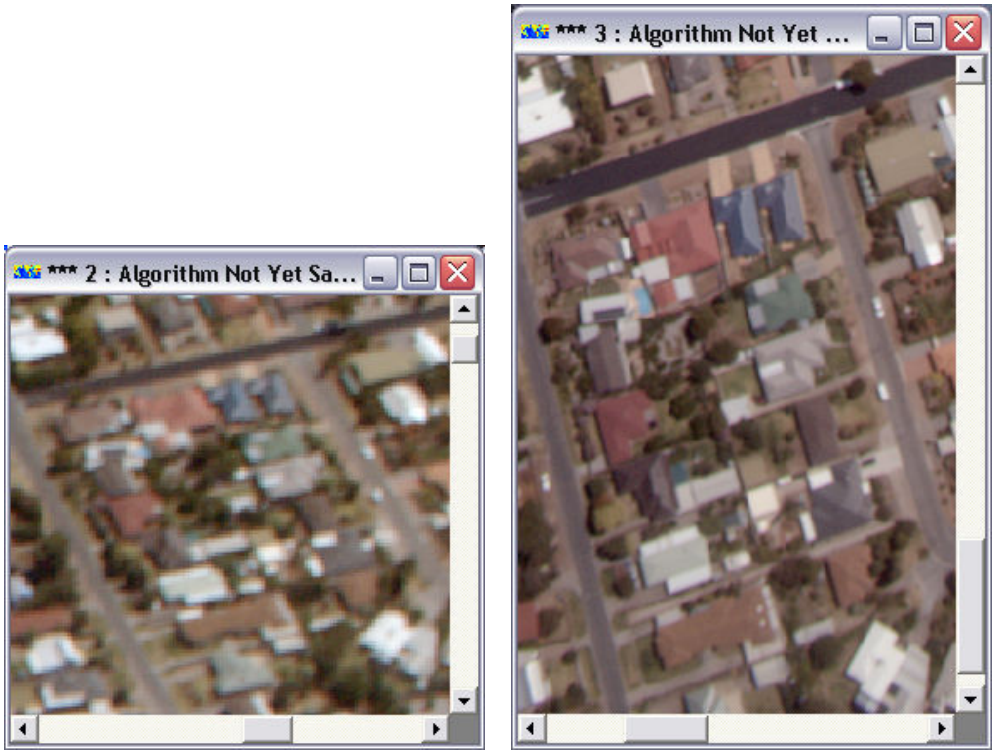


**Figure 18 Top part of frame 2489 (left) and bottom part of frame 2498 (right) demonstrating effects of different perspective, scale and resolution.**

Measuring the same objects at the top and bottom of frames gave scale differences in X and Y image coordinates[43]. The ratio in the X direction was 0.54. The ratio in the Y direction was 0.33. This meant that a one pixel object viewed near nadir was 0.54 pixels wide by 0.33 pixels in depth when viewed at the top.

Again by measuring objects of known size such as a cricket pitch[44] at top of frame 2194 and bottom of frame 2203 gave an approximate ground resolution. This gave a

---

topographic map. The easting of the top and bottom of the frame was estimated from features common to the frame and to a DEH orthorectified image. Trigonometry gave the reported results.

[43] In image coordinates.

[44] 1 chain or 22 yards or 20.22 metres long.

resolution in X of 60cm near the Brewster angle, and 32cm near the nadir, in agreement with the scale ratio.

### 3.3.5 Noise Measurement – Profile Method

An area of uniform appearance on deep water image 2092 was selected to test for noise (see figure 19). The assumption was that the bands would be very highly correlated and therefore noise would be easy to detect. Statistics were generated for the image (table 1).

| STATISTICS FOR DATASET: 2092_BGR.ers REGION: All | | | |
|---|---|---|---|
| | Band 1 | Band 2 | Band 3 |
| | Blue | Green | Red |
| Non-Null Cells | 2009709 | 2009709 | 2009709 |
| Minimum | 362.000 | 367.000 | 272.000 |
| Maximum | 707.000 | 663.000 | 362.000 |
| Mean | 554.961 | 539.177 | 312.631 |
| Median | 556.000 | 542.000 | 312.000 |
| Std. Dev. | 63.385 | 56.447 | 13.249 |
| Std. Dev. (n-1) | 63.385 | 56.447 | 13.249 |
| Corr. Eigenval. | 2.847 | 0.134 | 0.019 |
| Cov. Eigenval. | 7278.346 | 68.043 | 33.039 |
| | | | |
| Correlation Matrix | Band1 | Band2 | Band3 |
| Band1 | 1.000 | 0.981 | 0.894 |
| Band2 | 0.981 | 1.000 | 0.895 |
| Band3 | 0.894 | 0.895 | 1.000 |
| Determinant | 0.007 | | |
| | | | |
| Corr. Eigenvectors | PC1 | PC2 | PC3 |
| Band1 | 0.583 | -0.401 | -0.706 |
| Band2 | 0.583 | -0.398 | 0.708 |
| Band3 | 0.565 | 0.825 | -0.002 |
| | | | |
| Inv. of Corr. Ev. | PC1 | PC2 | PC3 |
| Band1 | 0.583 | 0.583 | 0.565 |
| Band2 | -0.401 | -0.398 | 0.825 |
| Band3 | -0.706 | 0.708 | -0.002 |
| | | | |
| Covariance Matrix | Band1 | Band2 | Band3 |
| Band1 | 4017.613 | 3509.431 | 750.963 |
| Band2 | 3509.431 | 3186.284 | 669.147 |
| Band3 | 750.963 | 669.147 | 175.531 |
| Determinant | 16362025.329 | | |

**Table 1 Statistics for frame 2092**

There was a high correlation between bands, as would be expected over relatively featureless water. The correlation matrix shows a high degree of correlation between all three bands. The blue and green bands show a very high correlation (0.981) as shown in figure 20.

The correlation between the blue and red bands and green and red bands are 0.894 and 0.895 respectively (figure 21). The lower correlation may be due to the tail of

pixel values due to the Perspex cover. The assumption that the bands are highly correlated was shown to be correct.

**Figure 19 Frame 2092 showing uncorrected (left), visually enhanced (centre) and balanced (right).**

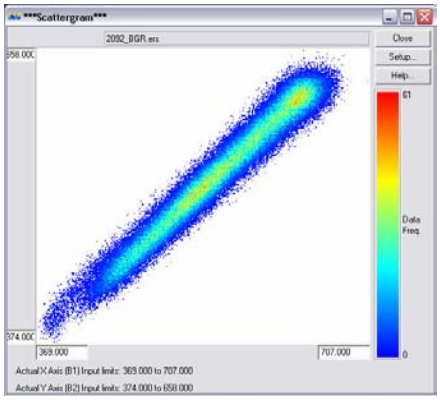


**Figure 20 Scatterplot of blue and green bands of frame 2092.**

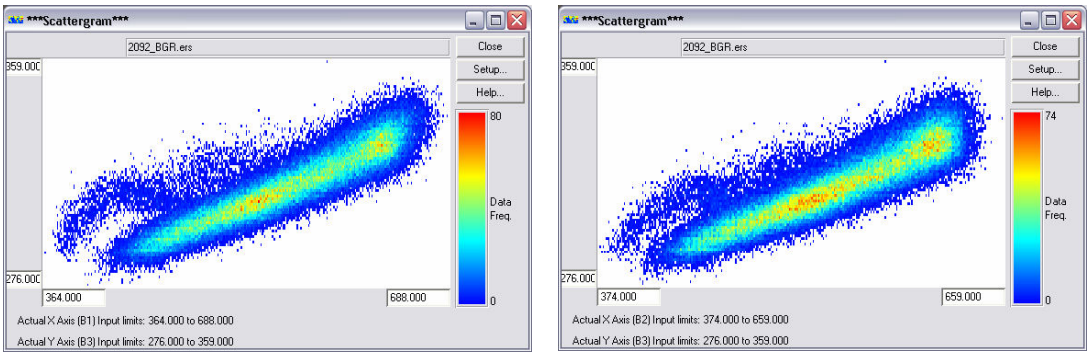


**Figure 21 Scatterplot of blue and red (left) and green and red (right) of frame 2092.**

For such a highly featureless image the assumption that the pixel values are highly correlated with adjacent pixel values within the same band can be made. Noise was defined as variation at the pixel level from the values of adjacent pixels. A profile line

was placed across the image from left to right. The pixel values were measured along the profile line and displayed. The left-of-centre image of the oil drop was used as a marker for the profile.

The first observation showed a marked vignetting[45] effect, especially on the right (northern) side of the image. This trend was noticeable in all three bands (see figure 22).

The second observation was the amount of variation in density number across each band. This is assumed to be noise. This was approximately 20 DN in each band. A related observation is that the spikes and troughs of values long the transect in each band do not match the spikes and troughs of the other bands, except where the oil drop artefact is located. This indicates that the noise is not correlated between bands (more on this later).

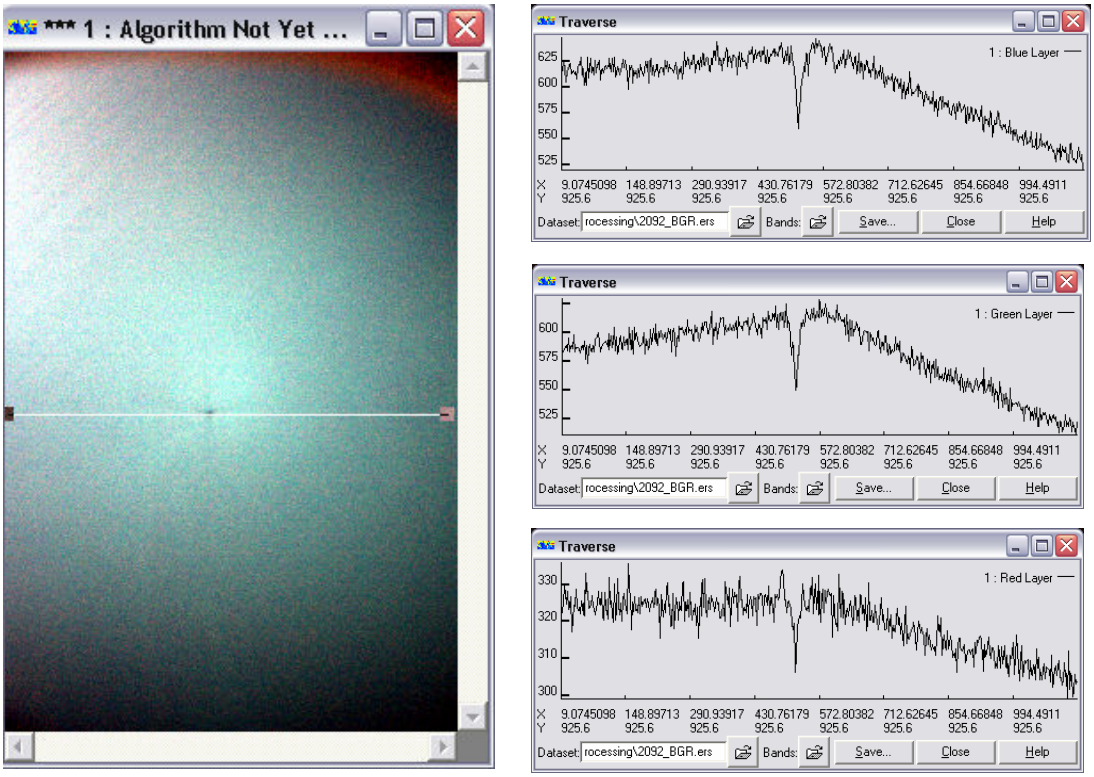


**Figure 22 Profile of Frame 2092 and traverse of the blue, green and red bands. X-axis is density number. Y-axis is distance in pixels from left registration column of image.**

[45] Cos4($\theta$) or "cosine fourth" law, where light falloff is roughly proportional to the fourth power of the cosine of $\theta$ (where $\theta$ is the angle off axis) (Wikipedia 2008). This is common on aerial photography and is usually corrected using an anti-vignetting lens filter, or using digital image processing to balance the image. An older method using film was dodging at the time of film printing, where the exposure time in the centre of the photography was reduced compared to the outer edges. This involved the photographer waving their hands over the centre of the photograph print as it was being exposed in the dark-room.

### 3.3.6 Removal of Vignetting

The vignetting effect was removed using the ERMapper balancing formula[46]. This had the effect of removing the brightness slope while leaving the noise untouched. The same spikes and troughs were visible on the balanced profiles as were on the original profiles for each band (figure 23).

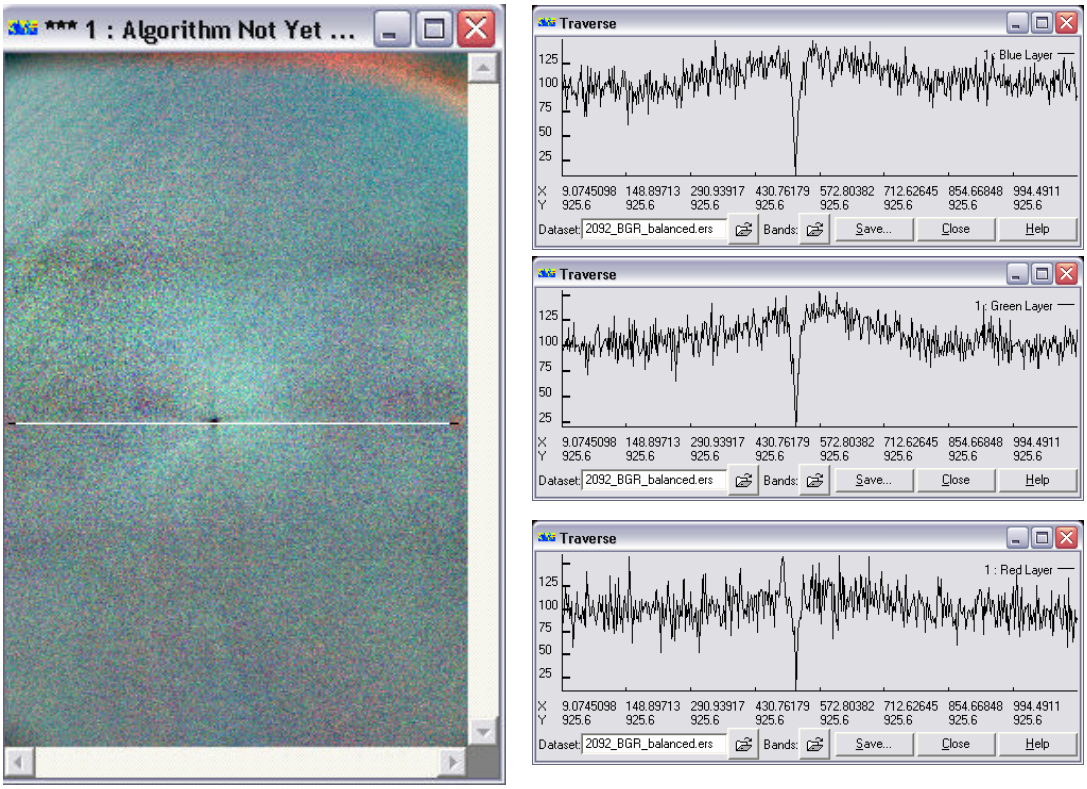


**Figure 23 Profiles after vignetting effect was removed.**

### 3.3.7 Noise Removal by Smoothing

The noise was removed using an 11 by 11 low pass filter on the image[47]. Not only did the filter remove most of the noise as seen on the traverse diagrams, but the image showed unexpected detail. Wave fronts were visible to the top left of the image (south-west) that were less conspicuous on the unsmoothed images. In addition benthic detail was visible in the bottom half of the image (east) (figure 24).

[46] This also had the effect of reducing the data from 10-bit radiometric resolution to 8-bit. It also expanded the noise amplitude.

[47] The size of the filter matrix was empirically derived by testing different matrix sizes. The 11 by 11 filter size seemed to give the best result.

This indicated that significant balancing and smoothing would be needed for image analysis of the data.

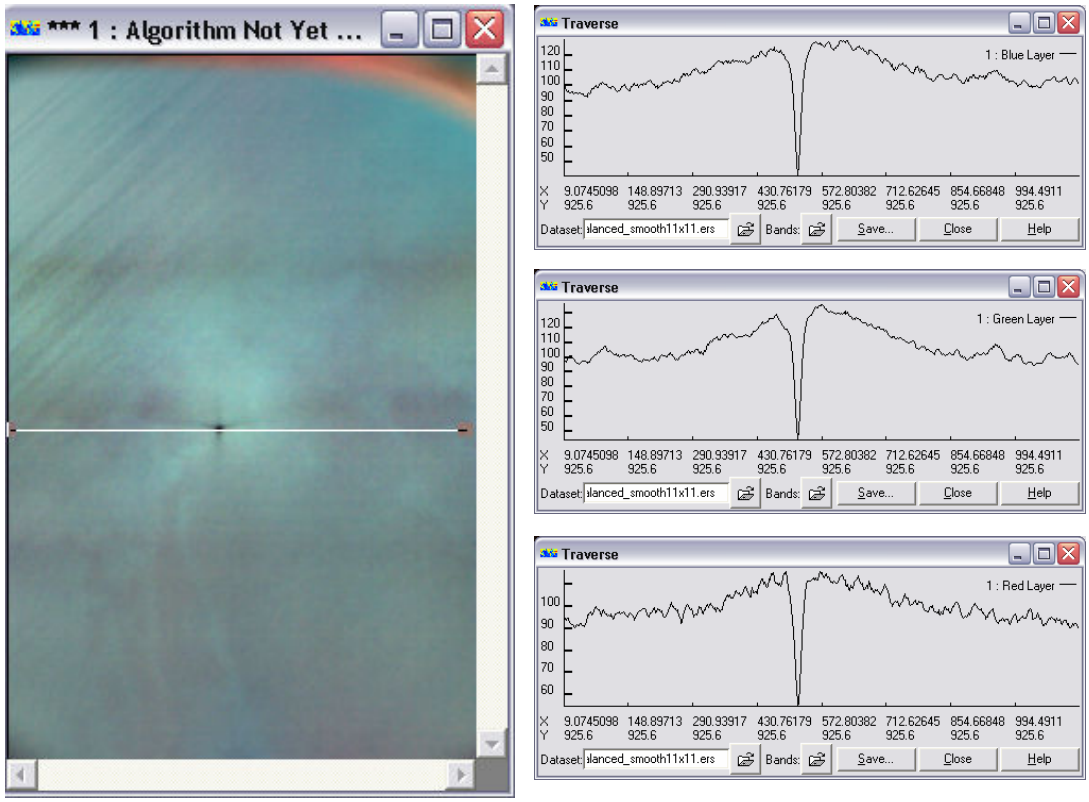


**Figure 24 Profiles after 11 by 11 low pass filter.**

### 3.3.8 Band Offset

The three bands captured during the mission were found to be not co-registered. A school cricket pitch was used to test band co-registration (figure 25). Bands were subtracted from each other; any misregistration would show as offset pixels or unexpected dark or light strips fringing an object.

This fringing effect was found to be the case (figure 26). Therefore the band pixels were not aligned by at least one pixel. This implies that any band arithmetic on the raw imagery could cause artefacts.

The band misregistration could be due to either the Bayer pattern (figure 27) of the RGB colour filters on the CMOS chip, or chromatic aberration of the camera lens (figure 28)[48].

[48] Other possible causes of band misregistration were ruled out. As this was a single shutter frame camera, differences due to mechanical movement (as with a line scanner such as

**Figure 25 Frame 2200 showing cricket pitch used to test for band registration (facing east).**

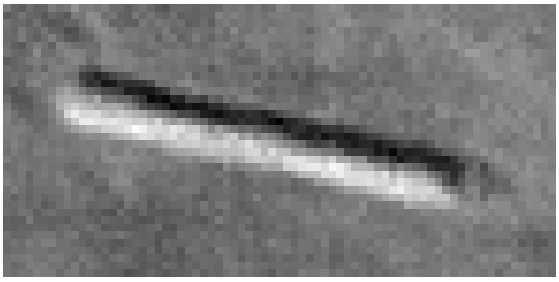

**Figure 26 Blue with red band subtracted, showing dark strip to the top of the cricket pitch (east), and a light strip to the bottom of the cricket pitch (west).**

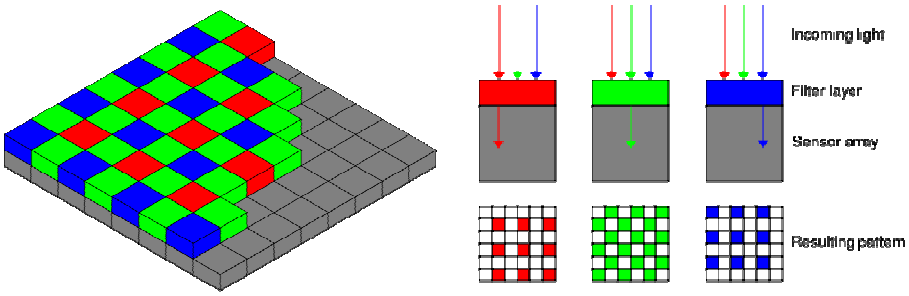


**Figure 27 Bayer pattern colour filter (Wikipedia 2008).**

Landsat Thematic Mapper or EO-1 Hyperion), sampling rates (as with push-broom scanner such as EO-1 ALI) or emulsion layers (such as colour film) could be ruled out.

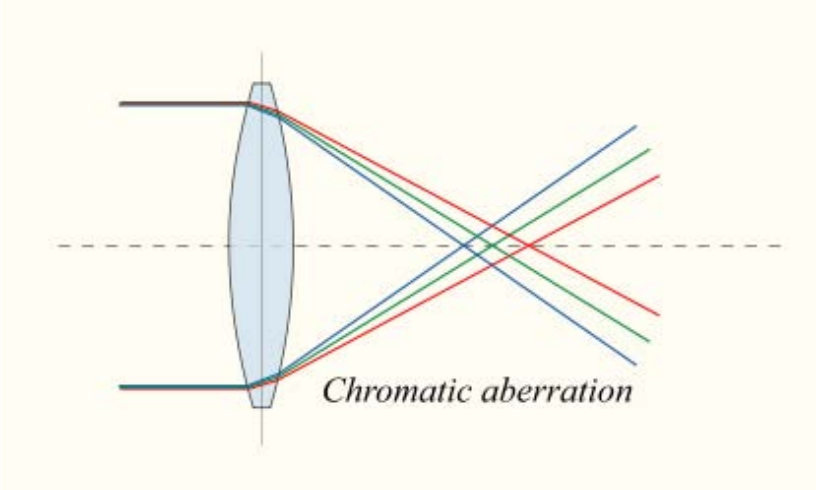


**Figure 28 Dispersion of light rays due to chromatic aberration (Wikipedia 2008).**

A simple test was devised to choose between these possibilities. If the effect was due to the Bayer pattern filter then the effect would be uniform over the image, and in the same direction and magnitude. However if the effect was due to chromatic aberration, then the effect would differ according to the direction away from the centre of the lens, with no aberration at the principal point of the lens.

To test this, the same cricket pitch was viewed on two frames, at the top of frame 2194 (figure 29), and at the bottom of frame 2203 (figure 30). The red and blue bands, having the most spectral separation and therefore the most chromatic aberration differences were combined.

The result showed a red edge on the top (missing blue) and a blue edge on the bottom (missing red) on both frames. As chromatic aberration would show blue above the cricket pitch on the top of frame, and blue below the cricket pitch on the bottom of frame, this showed that the misregistration effect was due to the Bayer pattern filter and not chromatic aberration.

The implication of this is that pixel based statistics and processing, especially at edges of features, is problematic. The feature each pixel represents is in a different location on the image depending on the band. The missing pixels are also interpolated to give a continuous image. This would give unreliable statistics.

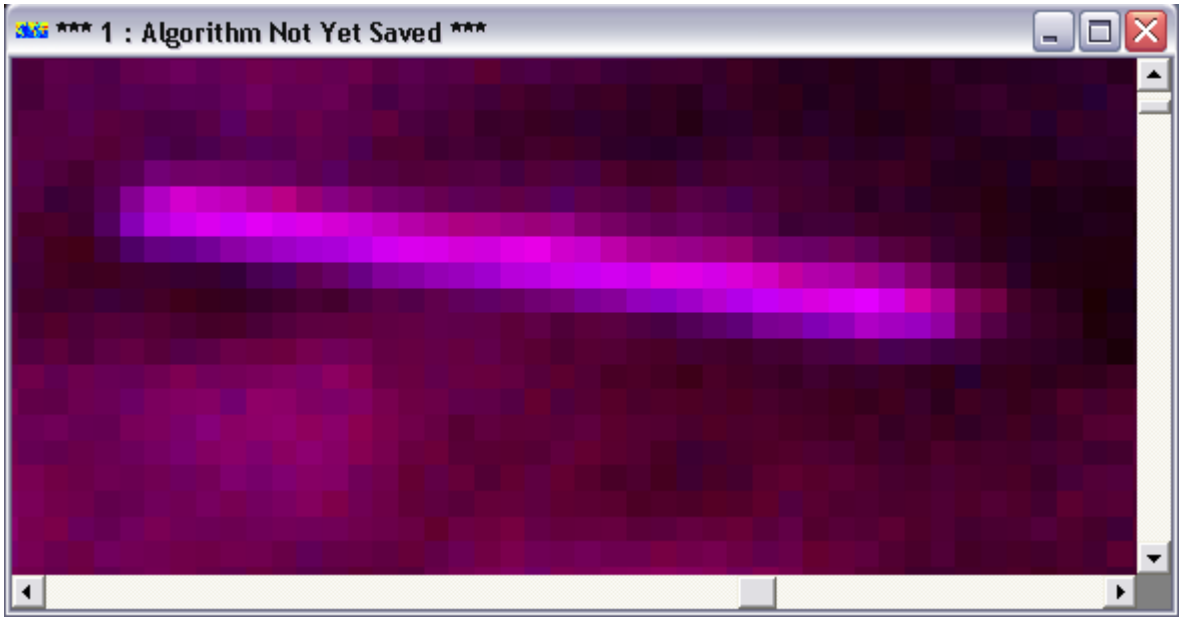


**Figure 29 Cricket pitch at top of frame 2194.**

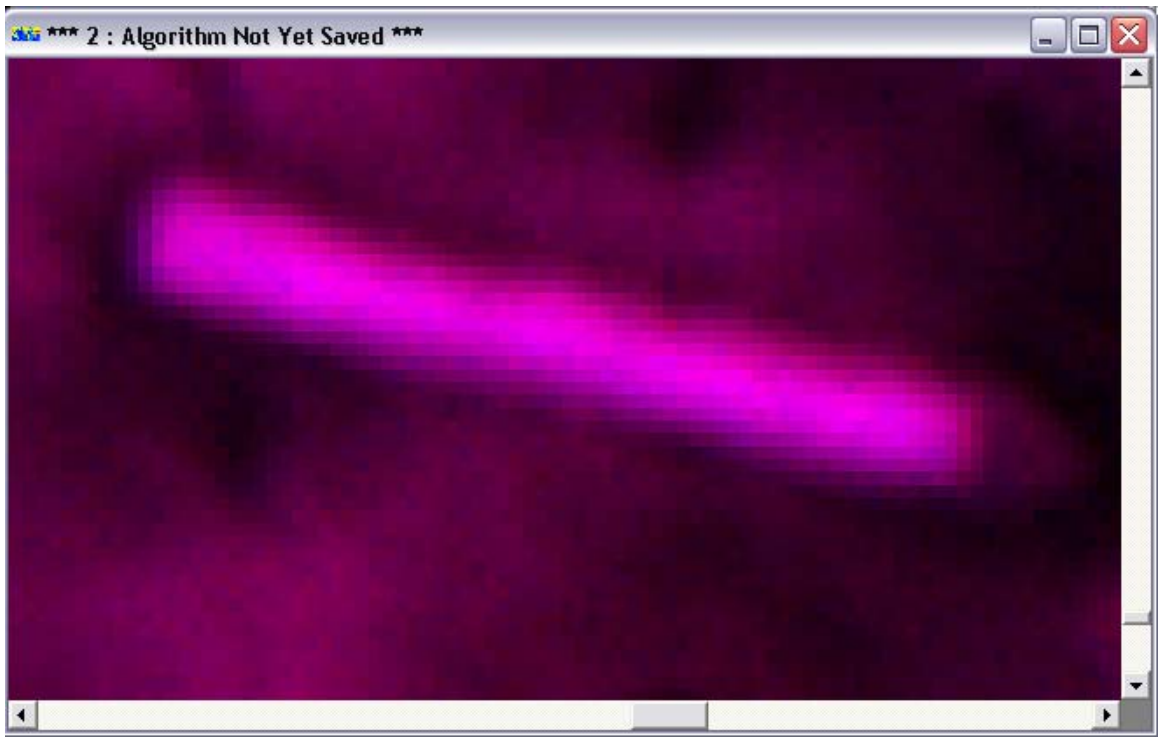


**Figure 30 Same cricket pitch at bottom of frame 2203.**

### 3.3.9 Contrast

Light and dark features in the sea are assumed to be substrate and seagrass respectively.

Having only vertically polarised imagery, there was nothing to compare it with to see if contrast improved. One method to overcome this apparent problem was the comparison of the same features imaged at approximately 16-20 degrees on one image, and at approximately 53 degrees on a related image. The photons imaged at 53 degrees would be purely vertically polarised, therefore the horizontally polarised surface reflection would be eliminated. Only the light reflected from the benthos would be imaged at that angle. The near nadir photons would be a combination of horizontal and vertically polarised photons from both the surface and the sea floor. Therefore the surface reflectance near nadir would reduce the contrast between benthic light and dark features.

Several point measurements of contrast between light and dark areas (figure 31) were undertaken at varying angles, and the density numbers compared. The results show that the contrast at 53 degrees is, on average, approximately 0.6 that of 16-20 degrees. The contrast was lower at the Brewster angle than near nadir.

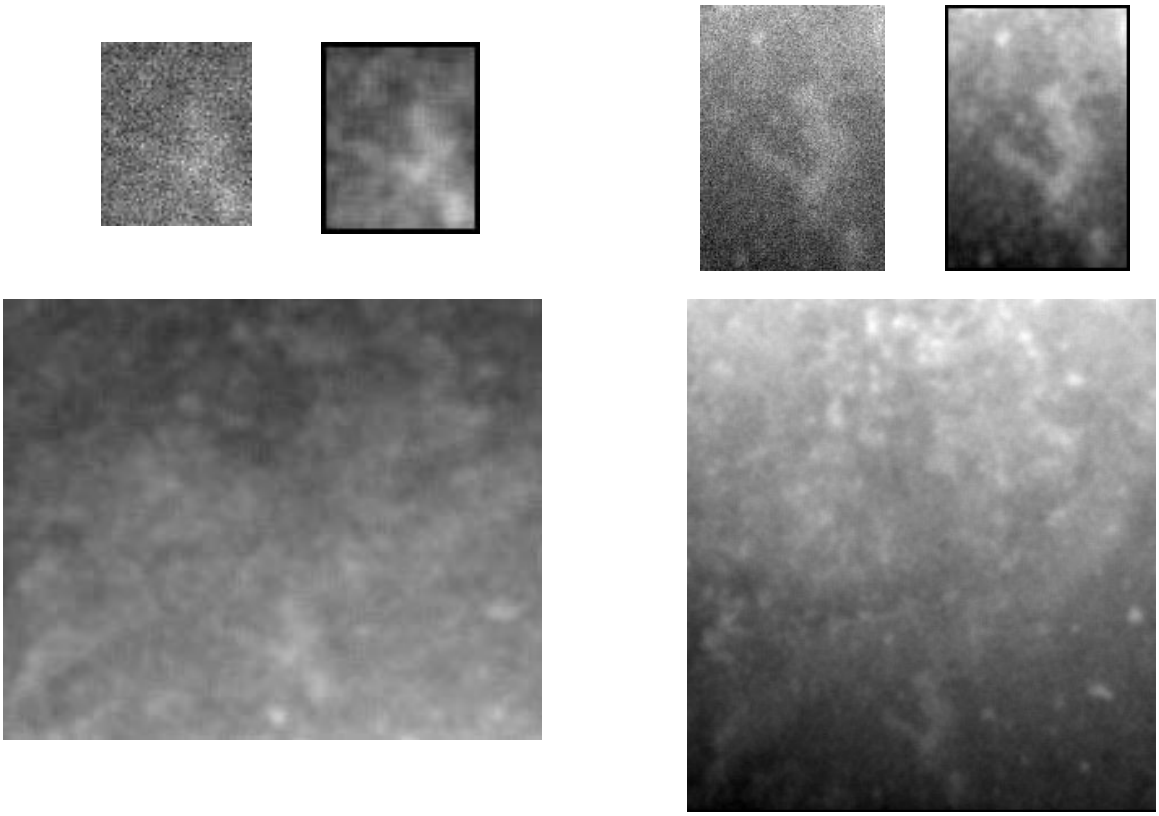

**Figure 31 Same feature at 53 degrees (left) and 16-20 degrees (right). The top images show the feature unenhanced (note the noise) and after smoothing. The bottom images show the location of the subsets and the vignetting effect in opposite directions.**

However this may not have been the result of polarisation differences. Another factor such as contrast decrease due to mixed pixels was tested for. This was the effect of scale differences between the top and bottom of the frame, with the top of frame pixels covering a larger area per pixel than those near the bottom of the frame.

A subset image was progressively resampled using bilinear interpolation. This was to simulate the effect of scale changes, changing pixels to mixed pixels (mixels). The resampling ratios where 1:1 (control image), 2:1 and 4:1. The histograms of the subset images were then compared (figure 32).

The result showed 0.75 change in contrast from the 1:1 image to the 4:1 image. This means that the apparent decrease in contrast due to the change in polarisation angle could be partially explained by the simple change of scale and resolution. Atmospheric absorption and scattering may have a minor effect on contrast.

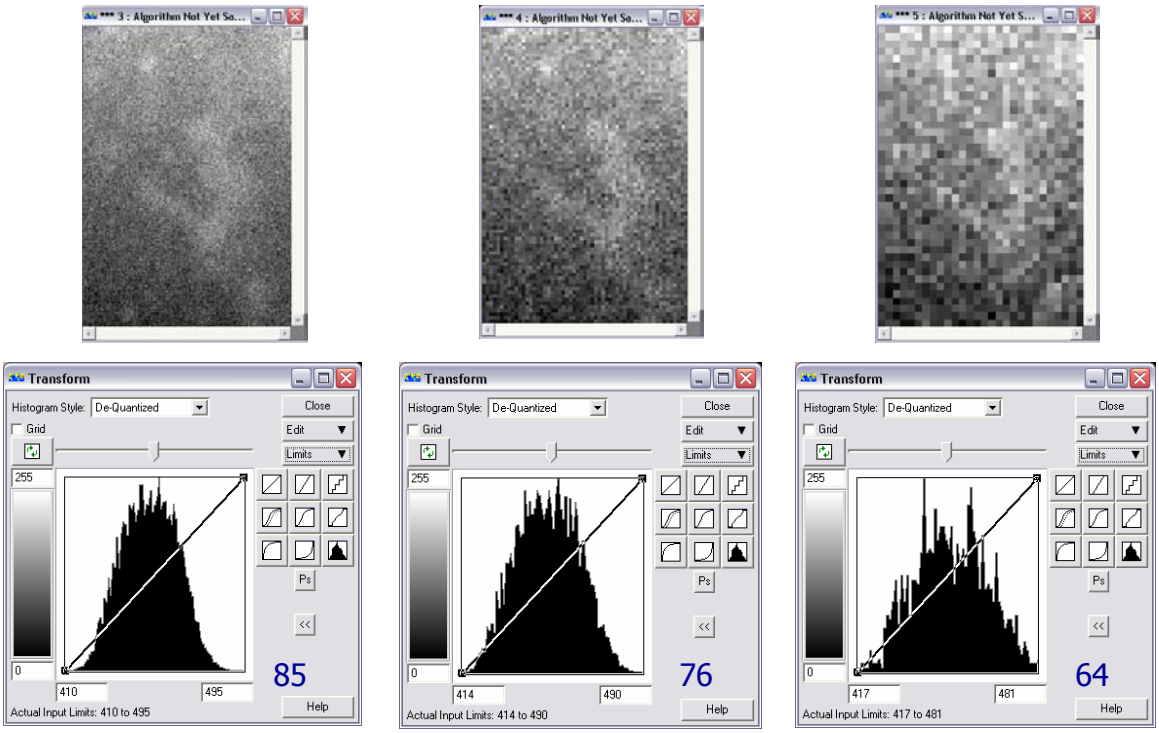


**Figure 32 Resampled subset images. 1:1 (left), 2:1 (centre), 4:1 (right). The histograms contracted in range. Range values in blue beside the histogram graph.**

## 3.4 Summary

### 3.4.1 Infra-Red imagery

The infra-red band showed minimal water depth penetration. This was expected due to the known infra-red absorption in water (Harrison and Jupp 1989)[49]. The initial use of the infra-red was to identify water surface features. The final experimental design was modified to use information in the visible spectrum for this purpose.

The co-temporal natural colour and infra-red frames with sun-glare towards the Brewster angle showed little difference in sun-glare intensity or extents. This showed that whatever effect or non-effect vertical polarisation had on removal of surface reflection, it was the same in both visible and infra-red parts of the spectrum.

Therefore for the full experiment the use of an infra-red band was not required. Furthermore, the use of a vertical polarisation filter did not improve the separation of seagrass and substrate as there was no signal from water depths where seagrass is found. A natural colour camera was considered sufficient for the data capture.

### 3.4.2 Natural Colour Imagery

The image analysis revealed the following information: cross-band pixels were not aligned, brightness values varied across the image due to vignetting, the data was very noisy, and analysis at pixel level would give spurious quantitative results.

The solutions proposed to overcome these problems were to use only a single band for analysis (preferably green for depth penetration), balance the image to remove vignetting effect, and smooth the image to remove noise.

Pixel level image arithmetic is therefore not advised on images derived from Bayer pattern filter CMOS chips. Any analysis should be at the whole-of-image or large region scale. Therefore the photointerpretation approach is preferred over the quantitative analysis approach for this type of imagery.

---

[49] However similar four band blue-green-red-infrared Vexcel Ultracam$_D$ imagery shows significant detail in water. One major difference between the two cameras is that the Vexcel UltracamD uses a panchromatic band to increase the apparent resolution of the multispectral bands.

The profile method of noise and vignetting evaluation and subsequent changes after balancing and smoothing was useful as a visualisation tool. This indicated that the images are inherently noisy, and need balancing and smoothing before visual interpretation is possible.

In terms of the effect of polarisation on contrast, higher oblique angles show lower contrast than near vertical angles. However this demonstrates nothing about polarisation, and may be a mixel effect.